Local density fluctuations, hyperuniformity, and order metrics

Salvatore Torquato
Department of Chemistry and Princeton Materials Institute, Princeton University, Princeton, New Jersey 08544, USA

Frank H. Stillinger
Department of Chemistry, Princeton University, Princeton, New Jersey 08544, USA

(Received 5 June 2003; published 29 October 2003; publisher error corrected 4 December 2003)

Questions concerning the properties and quantification of density fluctuations in point patterns continue to provide many theoretical challenges. The purpose of this paper is to characterize certain fundamental aspects of *local* density fluctuations associated with general point patterns in any space dimension d. Our specific objectives are to study the variance in the number of points contained within a regularly shaped window Ω of arbitrary size, and to further illuminate our understanding of *hyperuniform* systems, i.e., point patterns that do not possess infinite-wavelength fluctuations. For large windows, hyperuniform systems are characterized by a local variance that grows only as the surface area (rather than the volume) of the window. We derive two formulations for the number variance: (i) an ensemble-average formulation, which is valid for statistically homogeneous systems, and (ii) a volume-average formulation, applicable to a single realization of a general point pattern in the large-system limit. The ensemble-average formulation (which includes both real-space and Fourier representations) enables us to show that a homogeneous point pattern in a hyperuniform state is at a ''critical point'' of a type with appropriate scaling laws and critical exponents, but one in which the *direct correlation function* (rather than the pair correlation function) is long ranged. We also prove that the nonnegativity of the local number variance does not add a new realizability condition on the pair correlation. The volume-average formulation is superior for certain computational purposes, including optimization studies in which it is desired to find the particular point pattern with an extremal or targeted value of the variance. We prove that the simple periodic linear array yields the global minimum value of the average variance among all infinite one-dimensional hyperuniform patterns. We also evaluate the variance for common infinite periodic lattices as well as certain nonperiodic point patterns in one, two, and three dimensions for spherical windows, enabling us to rank-order the spatial patterns. Our results suggest that the local variance may serve as a useful order metric for general point patterns. Contrary to the conjecture that the lattices associated with the densest packing of congruent spheres have the smallest variance regardless of the space dimension, we show that for $d=3$, the body-centered cubic lattice has a smaller variance than the face-centered cubic lattice. Finally, for certain hyperuniform disordered point patterns, we evaluate the direct correlation function, structure factor, and associated critical exponents exactly.

DOI: 10.1103/PhysRevE.68.041113 PACS number(s): 05.20.−y, 61.20.Gy, 61.50.Ah

I. INTRODUCTION

The characterization of density fluctuations in many-particle systems is a problem of great fundamental interest in physical and biological sciences. In the context of liquids, it is well known that long-wavelength density fluctuations contain crucial thermodynamic and structural information about the system [1]. The measurement of galaxy density fluctuations is one of the most powerful ways to quantify and study the large-scale structure of the Universe [2,3]. Knowledge of density fluctuations in vibrated granular media has been used to probe the structure and collective motions of the grains [4]. Recently, the distribution of density fluctuations has been employed to reveal the fractal nature of structures within living cells [5].

Clearly, density fluctuations that occur on some arbitrary local length scale [4,6–10] provide considerably more information about the system than only long-wavelength fluctuations. Our main interest in this paper is to characterize certain fundamental aspects of *local* density fluctuations associated with general point patterns in any space dimension d. The point patterns may be thought as arising from the coordinates of the particles in a many-particle system, such as the molecules of a liquid, glass, quasicrystal or crystal, stars of a galaxy, grains of a granular packing, particles of a colloidal dispersion, or trees in a forest.

Consider an arbitrary point pattern in d-dimensional Euclidean space $\Re^d$. Let Ω represent a regular domain (window) in $\Re^d$ and $\mathbf{x}_0$ denote a configurational coordinate that specifies the centroid of the window Ω. The window will always have a fixed orientation. There is a variety of interesting questions that one could ask concerning the number of points contained within Ω. For example, how many points N_Ω are contained in Ω at some fixed coordinate $\mathbf{x}_0$? This question is a deterministic one if the point pattern is regular and may be a statistical one if the point pattern is irregular (see Fig. 1). How does the number of points contained within some initially chosen Ω at fixed coordinate $\mathbf{x}_0$ vary as the size of Ω is uniformly increased? How do the number of points within a fixed Ω fluctuate as $\mathbf{x}_0$ is varied?

For a Poisson point pattern, the statistics of the number of points contained within a regular domain are known exactly. For example, the number variance is given by

$$\langle N_\Omega^2\rangle - \langle N_\Omega\rangle^2 = \langle N_\Omega\rangle, \tag{1}$$

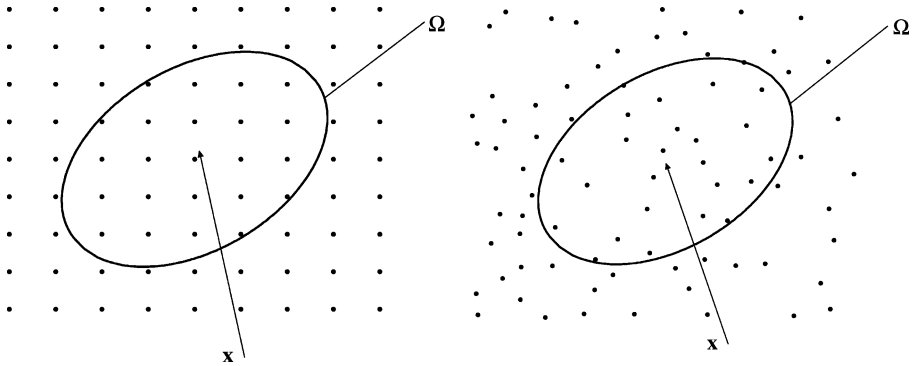

FIG. 1. Schematics indicating a regular domain or window Ω and its centroid $\mathbf{x}_0$ for two different point patterns. Left panel: A periodic point pattern. Right panel: An irregular point pattern. We will show that the statistics of the points contained within Ω for these two types of patterns are fundamentally different from one another.

where angular brackets denote an ensemble average. Letting Ω be a d-dimensional sphere of radius R and noting that $\langle N_\Omega \rangle$ is proportional to R^d leads to the result that the number variance grows as the sphere volume, i.e.,

$$\langle N_\Omega^2 \rangle - \langle N_\Omega \rangle^2 \propto R^d. \tag{2}$$

This result is not limited to Poisson point patterns. Indeed, a large class of correlated irregular point patterns obeys the variance formula (2), as we will discuss in Sec. II.

Can the variance grow more slowly than the volume of the domain or window? One can show that for any statistically homogeneous and isotropic point pattern, the variance cannot grow more slowly than the surface area of the domain, whether it is spherical or some other strictly convex shape [11,12]. Thus, it is natural to ask the following question: For what class of point pattern does the variance grow as the surface area? For a spherical domain, we want to identify the point patterns that obey the variance relation for large R,

$$\langle N_\Omega^2 \rangle - \langle N_\Omega \rangle^2 \sim R^{d-1}. \tag{3}$$

We will refer to such point patterns as ''hyperuniform'' systems because, as we will see, such systems do not possess infinite-wavelength fluctuations. (This is to be contrasted with ''hyposurficial'' systems, whose ''surface'' fluctuations vanish identically.) Additionally, it is of great interest to identify the particular point pattern that minimizes the amplitude (coefficient) of the fluctuations that obey Eq. (3) or achieves a targeted value of this coefficient.

Clearly, points arranged on a regular (periodic) lattice are hyperuniform. More generally, it is desired to know how the number of lattice points $N(R)$ contained within a spherical window of radius R varies as a function of R when the sphere is centered at $\mathbf{x}_0$. For simplicity, let us consider this question in two dimensions for points arranged on the square lattice and let the center of the circular window of radius R be positioned at a point (a_1,a_2) in the unit square. The answer to this query amounts to finding all of the integer solutions of

$$(n_1 - a_1)^2 + (n_2 - a_2)^2 \leqslant R^2, \tag{4}$$

a problem of interest in number theory [13,14]. This problem is directly related to the determination of the number of energy levels less than some fixed energy in integrable quantum systems [9]. It is clear that $N(R)$ asymptotically approaches the window area πR^2 for large R and unit density. The apparent ''random'' nature of $N(R)$ is beautifully illustrated in Fig. 2, which shows how the function $N(R) - \pi R^2$ grows with R.

It is considerably more challenging to identify nonperiodic point patterns, such as disordered and quasiperiodic ones, that are hyperuniform. The mathematical conditions that statistically homogeneous hyperuniform systems must obey (derived in Sec. II) are a necessary starting point in identifying such hyperuniform point patterns. These conditions, which include the counterintuitive property of a long-ranged ''direct'' correlation function, are determined from a general formula for the number variance of such systems, which is obtained in Sec. II. The fact that the direct correlation function of a hyperuniform pattern is long ranged is reminiscent of the behavior of the pair correlation function of a thermal system near its critical point. Indeed, we show that a statistically homogeneous point pattern in a hyperuniform state is at a ''critical point'' of a type with appropriate scaling laws and critical exponents. By deriving a Fourier representation of the local variance, it is also shown that the nonnegativity of the variance does not add a new realizability condition on the pair correlation function beyond the known ones.

To date, only a few statistically homogeneous and isotropic patterns have been rigorously shown to be hyperuniform. One of the aims of this paper is to identify other such hyperuniform examples, and to describe a procedure to find them systematically. This requires a formulation for the local vari-

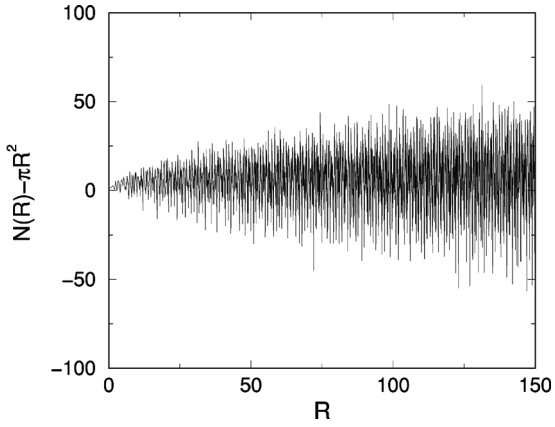

FIG. 2. The function $N(R) - \pi R^2$ vs R for the unit-spacing square lattice, using a circular window of radius R centered on a lattice point.

ance that can be applied to a single realization of any pattern, which is accomplished in Sec. III. In Sec. IV we prove that the simple periodic linear array yields the global minimum value of the average variance among all infinite one-dimensional hyperuniform patterns. Interestingly, we also show that the variance for large spherical windows enables us to rank-order common regular lattice and certain disordered point patterns in one, two, and three dimensions (see Secs. IV and V). Our results suggest that the local variance may provide a useful order metric for general point patterns (see Sec. VI). Contrary to the conjecture that the Bravais lattice associated with the densest packing of congruent spheres has the smallest variance regardless of the space dimension, we show that for $d=3$, the body-centered cubic lattice has a smaller variance than the face-centered cubic lattice. In Sec. V, we evaluate the direct correlation function, structure factor, and associated critical exponents exactly for certain hyperuniform disordered point patterns. Three appendixes provide analytical formulas for key geometrical quantities required for the theory, an evaluation of the variance for hard rods in equilibrium for large windows, and a discussion of a certain property of hyposurficial point patterns.

II. LOCAL VARIANCE FORMULA FOR REALIZATIONS OF STATISTICALLY HOMOGENEOUS SYSTEMS

A general expression for the local number variance for realizations of statistically homogeneous point patterns in d dimensions is derived. This is necessarily an ensemble-average formulation. We obtain both a real-space and a Fourier representation of the variance. From these results, we obtain formulas for asymptotically large windows. We show that a hyperuniform point pattern is at a type of critical point with appropriate scaling laws and critical exponents, but one in which the direct correlation function is long ranged.

A. Preliminaries

Consider N points with configuration $\mathbf{r}^N \equiv \mathbf{r}_1, \mathbf{r}_2, \ldots, \mathbf{r}_N$ in a volume V. The local number density at position $\mathbf{x}$ is given by

$$n(\mathbf{x}) = \sum_{i=1}^{N} \delta(\mathbf{x}-\mathbf{r}_i), \tag{5}$$

where $\delta(\mathbf{x})$ is the Dirac delta function. The point pattern is statistically characterized by the *specific* probability density function $P_N(\mathbf{r}^N)$, where $P_N(\mathbf{r}^N)d\mathbf{r}^N$ gives the probability of finding point 1 in volume element $d\mathbf{r}_1$ about $\mathbf{r}_1$, point 2 in volume element $d\mathbf{r}_2$ about $\mathbf{r}_2, \ldots,$ point N in volume element $d\mathbf{r}_N$ about $\mathbf{r}_N$. Thus, $P_N(\mathbf{r}^N)$ normalizes to unity and $d\mathbf{r}^N \equiv d\mathbf{r}_1, d\mathbf{r}_2, \ldots, d\mathbf{r}_N$ represents the Nd-dimensional volume element. The ensemble average of any function $f(\mathbf{r}^N)$ that depends on the configuration of points is given by

$$\langle f(\mathbf{r}^N)\rangle = \int_V \int_V \cdots \int_V f(\mathbf{r}^N) P_N(\mathbf{r}^N) d\mathbf{r}^N. \tag{6}$$

Because complete statistical information is usually not available, it is convenient to introduce the reduced *generic* density function $\rho_n(\mathbf{r}^n)$ $(n<N)$, defined as

$$\rho_n(\mathbf{r}^n) = \frac{N!}{(N-n)!} \int_V \cdots \int_V P_N(\mathbf{r}^N) d\mathbf{r}^{N-n}, \tag{7}$$

where $d\mathbf{r}^{N-n} \equiv d\mathbf{r}_{n+1} d\mathbf{r}_{n+2} \cdots d\mathbf{r}_N$. In words, $\rho_n(\mathbf{r}^n)d\mathbf{r}^n$ is proportional to the probability of finding *any* n particles $(n \leqslant N)$ with configuration $\mathbf{r}^n$ in volume element $d\mathbf{r}^n$. In light of its probabilistic nature, it is clear that $\rho_n(\mathbf{r}^n)$ is a non-negative quantity, i.e., $\rho_n(\mathbf{r}^n) \geqslant 0$, $\forall \mathbf{r}^n$.

For statistically homogeneous media, $\rho_n(\mathbf{r}^n)$ is translationally invariant and hence depends only on the relative displacements, say with respect to $\mathbf{r}_1$:

$$\rho_n(\mathbf{r}^n) = \rho_n(\mathbf{r}_{12}, \mathbf{r}_{13}, \ldots, \mathbf{r}_{1n}), \tag{8}$$

where $\mathbf{r}_{ij} = \mathbf{r}_j - \mathbf{r}_i$. In particular, the one-particle function ρ_1 is just equal to the constant *number density* of particles ρ, i.e.,

$$\rho_1(\mathbf{r}_1) = \rho \equiv \lim_{N,V\to\infty} \frac{N}{V}. \tag{9}$$

The limit indicated in Eq. (9) is referred to as the *thermodynamic limit*. Since our interest in this section is in statistically homogeneous point patterns, we now take the thermodynamic limit. It is convenient to define the so-called *n-particle correlation function*,

$$g_n(\mathbf{r}^n) = \frac{\rho_n(\mathbf{r}^n)}{\rho^n}. \tag{10}$$

In systems without long-range order and in which the particles are mutually far from one another (i.e., $r_{ij} = |\mathbf{r}_{ij}| \to \infty$, $1 \leqslant i < j \leqslant N$), $\rho_n(\mathbf{r}^n) \to \rho^n$ and we have from Eq. (10) that $g_n(\mathbf{r}^n) \to 1$. Thus, the deviation of g_n from unity provides a measure of the degree of spatial correlation between the particles, with unity corresponding to no spatial correlation.

The important two-particle quantity

$$g_2(\mathbf{r}_{12}) = \frac{\rho_2(\mathbf{r}_{12})}{\rho^2} \tag{11}$$

is usually referred to as the *pair correlation function*. The *total correlation function* $h(\mathbf{r}_{12})$ is defined as

$$h(\mathbf{r}_{12}) = g_2(\mathbf{r}_{12}) - 1, \tag{12}$$

and thus is a function that is zero when there are no spatial correlations in the system. When the system is both statistically homogeneous and isotropic, the pair correlation function depends on the radial distance r_{12} only, i.e.,

$$g_2(\mathbf{r}_{12}) = g_2(r_{12}), \tag{13}$$

and is referred to as the radial distribution function. From Eq. (11), we see that $\rho s_1(r) g_2(r) dr$ is proportional to the *conditional probability* of finding a particle center in a

spherical shell of volume $s_1(r)dr$, given that there is another at the origin. Here $s_1(r)$ is the surface area of a d-dimensional sphere of radius r, which is given by

$$s_1(r)=\frac{2\pi^{d/2}r^{d-1}}{\Gamma(d/2)}, \tag{14}$$

where $\Gamma(x)$ is the gamma function. Hence, for a finite system, integrating $(N-1)g_2(r)/V$ over the volume yields $N-1$, i.e., all the particles except the one at the origin.

Observe that the structure factor $S(\mathbf{k})$ is related to the Fourier transform of $h(\mathbf{r})$, denoted by $\tilde{h}(\mathbf{k})$, via the expression

$$S(\mathbf{k})=1+\rho\tilde{h}(\mathbf{k}). \tag{15}$$

The Fourier transform of some absolutely integrable function $f(\mathbf{r})$ in d dimensions is given by

$$\tilde{f}(\mathbf{k})=\int f(\mathbf{r})e^{-i\mathbf{k}\cdot\mathbf{r}}d\mathbf{r}, \tag{16}$$

and the associated inverse operation is defined by

$$f(\mathbf{r})=\frac{1}{(2\pi)^d}\int \tilde{f}(\mathbf{k})e^{i\mathbf{k}\cdot\mathbf{r}}d\mathbf{k}, \tag{17}$$

where $\mathbf{k}$ is the wave vector. It is well known that the structure factor is proportional to the scattered intensity of radiation from a system of points and thus is obtainable from a scattering experiment. An important property of the structure factor is that it must be non-negative for all $\mathbf{k}$, i.e.,

$$S(\mathbf{k})\geqslant 0 \quad \forall\mathbf{k}. \tag{18}$$

B. General variance formulas

Let $\mathbf{R}$ symbolize the parameters that characterize the geometry of the window Ω. For example, in the case of an ellipsoidal window, $\mathbf{R}$ would represent the semiaxes of the ellipsoid. Let us introduce the window indicator function

$$w(\mathbf{x}-\mathbf{x}_0;\mathbf{R})=\begin{cases}1, & \mathbf{x}\in\Omega\\ 0, & \mathbf{x}\notin\Omega,\end{cases} \tag{19}$$

for a window with a configurational coordinate $\mathbf{x}_0$. The number of points N_Ω within the window at $\mathbf{x}_0$, which we henceforth denote by $N(\mathbf{x}_0;\mathbf{R})$, is given by

$$\begin{aligned}N(\mathbf{x}_0;\mathbf{R})&=\int_V n(\mathbf{x})w(\mathbf{x}-\mathbf{x}_0;\mathbf{R})d\mathbf{x}\\ &=\sum_{i=1}^{N}\int_V \delta(\mathbf{x}-\mathbf{r}_i)w(\mathbf{x}-\mathbf{x}_0;\mathbf{R})d\mathbf{x}\\ &=\sum_{i=1}^{N} w(\mathbf{r}_i-\mathbf{x}_0;\mathbf{R}).\end{aligned} \tag{20}$$

Therefore, the average number of points contained within the window in a realization of the ensemble is

$$\begin{aligned}\langle N(\mathbf{R})\rangle&=\int_V\sum_{i=1}^{N} w(\mathbf{r}_i-\mathbf{x}_0;\mathbf{R})P_N(\mathbf{r}^N)d\mathbf{r}^N\\ &=\int_V\rho_1(\mathbf{r}_1)w(\mathbf{r}_1-\mathbf{x}_0;\mathbf{R})d\mathbf{r}_1\\ &=\rho\int_{\Re^d}w(\mathbf{r};\mathbf{R})d\mathbf{r}\\ &=\rho v_1(\mathbf{R}),\end{aligned} \tag{21}$$

where $v_1(\mathbf{R})$ is the volume of a window with geometric parameters $\mathbf{R}$. Note that translational invariance of the point pattern, invoked in the third line of relation (21), renders the average $\langle N(\mathbf{R})\rangle$ independent of the window coordinate $\mathbf{x}_0$.

Similarly, ensemble averaging the square of Eq. (20) and using relation (21) gives the local number variance as

$$\begin{aligned}\langle N^2(\mathbf{R})\rangle-\langle N(\mathbf{R})\rangle^2&=\int_V\rho_1(\mathbf{r}_1)w(\mathbf{r}_1-\mathbf{x}_0;\mathbf{R})d\mathbf{r}_1+\int_V\int_V[\rho_2(\mathbf{r}_1,\mathbf{r}_2)-\rho_1(\mathbf{r}_1)\rho_1(\mathbf{r}_2)]w(\mathbf{r}_1-\mathbf{x}_0;\mathbf{R})w(\mathbf{r}_2-\mathbf{x}_0;\mathbf{R})d\mathbf{r}_1d\mathbf{r}_2\\ &=\langle N(\mathbf{R})\rangle\left[1+\rho\int_{\Re^d}h(\mathbf{r})\alpha(\mathbf{r};\mathbf{R})d\mathbf{r}\right],\end{aligned} \tag{22}$$

where $h(\mathbf{r})$ is the total correlation function defined by Eq. (12),

$$\alpha(\mathbf{r};\mathbf{R})=\frac{v_2^{\mathrm{int}}(\mathbf{r};\mathbf{R})}{v_1(\mathbf{R})}, \tag{23}$$

and

$$v_2^{\mathrm{int}}(\mathbf{r};\mathbf{R})=\int_{\Re^d}w(\mathbf{r}_1-\mathbf{x}_0;\mathbf{R})w(\mathbf{r}_2-\mathbf{x}_0;\mathbf{R})d\mathbf{x}_0 \tag{24}$$

is the intersection volume of two windows (with the same orientations) whose centroids are separated by the displacement vector $\mathbf{r}=\mathbf{r}_1-\mathbf{r}_2$ [15]. Appendix A provides explicit analytical formulas for the intersection volume for spherical windows in arbitrary dimension d. As before, statistical ho-

mogeneity, invoked in the second line of Eq. (22), renders the variance independent of $\mathbf{x}_0$.

Remarks.

(1) Formula (22) was previously derived by Landau and Lifschitz [16], although they did not explicitly indicate the scaled intersection volume function $\alpha(\mathbf{r};\mathbf{R})$. Martin and Yalcin [17] derived the analogous formula for charge fluctuations in classical Coulombic systems.

(2) The local variance formula (22) is closely related to one associated with the local volume fraction fluctuations in two-phase random heterogeneous materials [15,18]. Both formulas involve the scaled intersection volume function $\alpha(\mathbf{r};\mathbf{R})$. The essential difference is that the variance for local volume fraction fluctuations involves a different correlation function from $h(\mathbf{r})$, namely, the probability of finding two points, separated by a displacement $\mathbf{r}$, both in the same phase.

(3) The existence of the integral in Eq. (22) requires that the product $h(\mathbf{r})\alpha(\mathbf{r};\mathbf{R})$ be integrable. For finite size windows, this will be the case for bounded $h(\mathbf{r})$ because $\alpha(\mathbf{r};\mathbf{R})$ is zero beyond a finite distance. For infinitely large windows, $\alpha(\mathbf{r};\mathbf{R})=1$, and integrability requires that $h(\mathbf{r})$ decays faster than $|\mathbf{r}|^{-d+\epsilon}$ for some $\epsilon>0$. For systems in thermal equilibrium, this will be the case for pure phases away from critical points. The structure factor S($\mathbf{k}$) [defined by Eq. (15)] at $\mathbf{k}=\mathbf{0}$ diverges as a thermal critical point is approached, implying that $h(\mathbf{r})$ becomes long ranged, i.e., decays slower than $|\mathbf{r}|^{-d}$ [19].

An outstanding question in statistical physics is: What are the existence conditions for a valid (i.e., physically realizable) total correlation function $h(\mathbf{r})$ [20] of a point process at fixed density ρ? The generalization of the Wiener-Khinchtine theorem for multidimensional spatial stochastic processes [21] states a necessary and sufficient condition for the existence of an autocovariance function of a general stochastically continuous homogeneous process is that it has a spectral (Fourier-Stieltjes) representation with a non-negative bounded measure. If the autocovariance is absolutely integrable, this implies that its Fourier transform must be nonnegative. The total correlation function $h(\mathbf{r})$ is the nontrivial part of the autocovariance function for a point process, i.e., it excludes the δ function at the origin. The fact that $h(\mathbf{r})$ comes from a statistically homogeneous point process, however, would further restrict the existence conditions on $h(\mathbf{r})$ beyond the Wiener-Khinchtine condition, which amounts to the non-negativity of the structure factor. Obviously, besides the condition that $S(\mathbf{k})\geqslant\mathbf{0}$, we have the pointwise condition $h(\mathbf{r})\geqslant -1$ for all $\mathbf{r}$. The determination of other realizability conditions on $h(\mathbf{r})$ is a open question [20].

Thus, it is interesting to inquire whether the nonnegativity of the local number variance, given by formula (22), is a new condition on $h(\mathbf{r})$ beyond the non-negativity of the structure factor $S(\mathbf{k})$. As we now prove, the answer is no. By Parseval's theorem for Fourier transforms [22], we can rewrite the general variance formula (22) for an arbitrarily shaped (regular) window as

$$\langle N^2(\mathbf{R})\rangle-\langle N(\mathbf{R})\rangle^2 = \langle N(\mathbf{R})\rangle\left[1+\frac{\rho}{(2\pi)^d}\int \tilde{h}(\mathbf{k})\tilde{\alpha}(\mathbf{k};\mathbf{R})d\mathbf{k}\right], \quad (25)$$

where

$$\tilde{\alpha}(\mathbf{k};\mathbf{R})=\frac{\tilde{w}^2(\mathbf{k};\mathbf{R})}{v_1(\mathbf{R})}\geqslant 0 \quad (26)$$

is the Fourier transform of the scaled intersection volume function (23) and $\tilde{w}(\mathbf{k};\mathbf{R})$ is the Fourier transform of the window indicator function (19). Again, by Parseval's theorem

$$\frac{1}{(2\pi)^d}\int \tilde{\alpha}(\mathbf{k};\mathbf{R})d\mathbf{k}=\frac{1}{v_1(\mathbf{R})}\int w^2(\mathbf{r})d\mathbf{r}=1. \quad (27)$$

Finally, utilizing definition (15) of the structure factor, we arrive at the Fourier representation of the number variance:

$$\langle N^2(\mathbf{R})\rangle-\langle N(\mathbf{R})\rangle^2=\langle N(\mathbf{R})\rangle\left[\frac{1}{(2\pi)^d}\int S(\mathbf{k})\tilde{\alpha}(\mathbf{k};\mathbf{R})d\mathbf{k}\right]. \quad (28)$$

Interestingly, we see that the variance formula can be rewritten in terms of the structure factor and the non-negative function $\tilde{\alpha}(\mathbf{k};\mathbf{R})$, the Fourier transform of the scaled intersection volume function $\alpha(\mathbf{r};\mathbf{R})$: a purely geometric quantity. Since the latter is independent of the correlation function $h(\mathbf{r})$, we conclude that the non-negativity of the number variance does not introduce a new realizability condition on $h(\mathbf{r})$.

Remarks.

(1) Given the Fourier representation formula (28), it is simple to prove that the local number variance is strictly positive for any $v_1(\mathbf{R})>\mathbf{0}$. Both the functions $\tilde{\alpha}(\mathbf{k};\mathbf{R})$ and $S(\mathbf{k})$ are non-negative. Therefore, because the non-negative integrand of formula (28) cannot be zero for all $\mathbf{k}$, it immediately follows that the local variance is strictly positive for any statistically homogeneous point pattern whenever $v_1(\mathbf{R})>\mathbf{0}$, i.e.,

$$\langle N^2(\mathbf{R})\rangle-\langle N(\mathbf{R})\rangle^2>0. \quad (29)$$

(2) Let the window grow infinitely large in a self-similar (i.e., shape- and orientation-preserving) fashion. In this limit, which we will denote simply by $v_1(\mathbf{R})\to\infty$, the function $\tilde{\alpha}(\mathbf{k};\mathbf{R})$ appearing in Eq. (28) tends to $(2\pi)^d\delta(\mathbf{k})$, where $\delta(\mathbf{k})$ is a d-dimensional Dirac delta function, and therefore dividing variance (28) by $\langle N(\mathbf{R})\rangle$ yields

$$\lim_{v_1(\mathbf{R})\to\infty}\frac{\langle N^2(\mathbf{R})\rangle-\langle N(\mathbf{R})\rangle^2}{\langle N(\mathbf{R})\rangle}=S(\mathbf{k}=\mathbf{0})=1+\rho\int_{\Re^d}h(\mathbf{r})d\mathbf{r}. \quad (30)$$

Observe also that the form of the scaled variance (30) for infinitely large windows (or infinite-wavelength limit) is identical to that for equilibrium "open" systems, i.e., grand canonical ensemble, in the infinite-system limit. It is well known that the variance in the latter instance is related to thermodynamic compressibilities or susceptibilities [1]. The important distinction is that result (30) is derived by considering window fluctuations in an infinite "closed" possibly

nonequilibrium system. When the point pattern comes from a statistically homogeneous equilibrium ensemble, one can interpret the fluctuations as arising from differences in the point patterns in the ensemble members for a fixed window position or, equivalently, from moving the asymptotically large window from point to point in a *single* system. The latter scenario can be viewed as corresponding to density fluctuations associated with an open system.

C. Asymptotic variance formulas

Here we apply the previous results for statistically homogeneous point patterns to obtain asymptotic results for large windows. The conditions under which these expressions yield variances that only grow as the surface area of Ω are determined. These conditions can be expressed in terms of spatial moments of the total correlation function $h(\mathbf{r})$. For simplicity, we first consider the case of spherical windows, but we show that the results apply as well to nonspherical windows.

Many of our subsequent results will be given for a d-dimensional spherical window of radius R centered at position $\mathbf{x}_0$. The window indicator function becomes

$$w(|\mathbf{x}-\mathbf{x}_0|;R)=\Theta(R-|\mathbf{x}-\mathbf{x}_0|), \tag{31}$$

where $\Theta(x)$ is the Heaviside step function,

$$\Theta(x)=\begin{cases}0, & x<0\\ 1, & x\geqslant 0.\end{cases} \tag{32}$$

Therefore, the function $v_1(\mathbf{R})$, defined in relation (21), becomes the volume of a spherical window of radius R given by

$$v_1(R)=\frac{\pi^{d/2}}{\Gamma(1+d/2)}R^d. \tag{33}$$

It is convenient to introduce a dimensionless density ϕ defined by

$$\phi=\rho v_1(D/2)=\rho\frac{\pi^{d/2}}{2^d\Gamma(1+d/2)}D^d, \tag{34}$$

where D is a characteristic microscopic length scale of the system, e.g., the mean nearest-neighbor distance between the points.

Substitution of expansion (A14) for the scaled intersection volume $\alpha(r;R)$ into Eq. (22), and assuming that the resulting integrals separately converge, yields the variance formula for large R as

$$\langle N^2(R)\rangle-\langle N(R)\rangle^2=2^d\phi\left[A\left(\frac{R}{D}\right)^d+B\left(\frac{R}{D}\right)^{d-1}+\ell\left(\frac{R}{D}\right)^{d-1}\right], \tag{35}$$

where A and B are the asymptotic constants given by

$$A=1+\rho\int_{\Re^d}h(\mathbf{r})d\mathbf{r}=1+\frac{\phi}{v_1(D/2)}\int_{\Re^d}h(\mathbf{r})d\mathbf{r}, \tag{36}$$

$$B=-\frac{\phi d\Gamma(d/2)}{2Dv_1(D/2)\Gamma\left(\frac{d+1}{2}\right)\Gamma\left(\frac{1}{2}\right)}\int_{\Re^d}h(\mathbf{r})r\,d\mathbf{r}, \tag{37}$$

and $\ell(x)$ signifies terms of lower order than x [23]. In what follows, the asymptotic constants A and B will generically be referred to as "volume" and "surface-area" coefficients for point patterns in *any* dimension.

Remarks.

(1) Observe that the volume coefficient A is equal to the non-negative structure factor in the limit that the wave number approaches zero, i.e.,

$$A=\lim_{|\mathbf{k}|\to 0}S(\mathbf{k})=1+\rho\int_{\Re^d}h(\mathbf{r})d\mathbf{r}\geqslant 0, \tag{38}$$

where $S(\mathbf{k})$ is defined by Eq. (15) for any dimension. Consistent with our earlier observations about relation (30), we see that A is the dominant term for very large windows and indeed is the only contribution for infinitely large windows. It is well known that point patterns generated from equilibrium molecular systems with a wide class of interaction potentials (e.g., hard-sphere, square-well, and Lennard-Jones interactions) yield positive values of A in gaseous, liquid, and many solid states. Indeed, A will be positive for any equilibrium system possessing a positive compressibility. This class of systems includes correlated equilibrium particle systems, an example of which is discussed in Appendix B. The coefficient A will also be positive for a wide class of nonequilibrium point patterns. One nonequilibrium example is the so-called random sequential addition process [15]. To summarize, there is an enormously large class of point patterns in which A is nonzero.

(2) Because the local variance is a strictly positive quantity for $R>0$ [cf. Eq. (29)], we have from Eq. (35) that for very large windows

$$A\left(\frac{R}{D}\right)^d+B\left(\frac{R}{D}\right)^{d-1}>0. \tag{39}$$

The crucial point to observe is that if the volume coefficient A identically vanishes, then the second term within the brackets of Eq. (35) dominates, and we have the condition

$$B>0, \tag{40}$$

where we have used the fact that the variance cannot grow more slowly than R^{d-1}, i.e., the surface area of the window [11]. We will refer to a system in which

$$A=\lim_{|\mathbf{k}|\to 0}S(\mathbf{k})=0 \tag{41}$$

as a "hyperuniform" system. Such point patterns do not possess infinite-wavelength fluctuations. In a recent cosmological study [3], the term "superhomogeneous" has been used to describe such systems. Note that for a one-dimensional hyperuniform system, the variance is exactly (not asymptotically) given by

$$\langle N^2(R)\rangle - \langle N(R)\rangle^2 = 2\phi B, \tag{42}$$

where B is given by Eq. (37) with $d=1$, implying that the fluctuations are bounded, i.e., do not grow with R [24].

(3) By contrast, we will refer to a point pattern in which the surface-area coefficient vanishes ($B=0$) as a "hyposurficial" system. A homogeneous Poisson point pattern is a simple example of such a system. Inequality (39) in conjunction with the fact that the variance cannot grow more slowly than the surface area of a spherical (or strictly convex) window for statistically homogeneous and isotropic point patterns [11], enables us to conclude that such a system cannot simultaneously be hyperuniform and hyposurficial, i.e., the volume coefficient A [cf. Eq. (36)] and surface-area coefficient B [cf. Eq. (37)] cannot both be zero. In Appendix C, we examine the question of how small the volume coefficient A can be made if the point pattern is hyposurficial.

(4) Observe also that the asymptotic variance formula (35) and the analysis leading to condition (40) are valid for any statistically homogeneous point pattern. Now if we further assume that the point pattern is statistically isotropic, then the volume coefficient (36) and surface-area coefficient (37) can be expressed in terms of certain moments of h, namely,

$$A = 1 + d2^d \phi \langle x^{d-1}\rangle, \tag{43}$$

$$B = -\frac{d^2 2^{d-1}\Gamma(d/2)}{\Gamma\left(\frac{d+1}{2}\right)\Gamma\left(\frac{1}{2}\right)}\phi\langle x^d\rangle, \tag{44}$$

where

$$\langle x^n\rangle = \int_0^\infty x^n h(x)dx \tag{45}$$

is the nth moment of the total correlation function $h(x)$ and $x=r/D$ is a dimensionless distance. Following the previous analysis, we see that if $A=0$, then the condition for the variance to grow as the surface area implies that the dth moment of h must be strictly negative, i.e.,

$$\langle x^d\rangle < 0. \tag{46}$$

D. Direct correlation function and new critical exponents

The *direct* correlation function $c(\mathbf{r})$ of a hyperuniform system behaves in an unconventional manner. In real space, this function is defined by the Ornstein-Zernike equation

$$h(\mathbf{r}) = c(\mathbf{r}) + \rho\int_{\Re^d} h(\mathbf{r}-\mathbf{r}')c(\mathbf{r})d\mathbf{r}'. \tag{47}$$

This relation has primarily been used to study liquids in equilibrium [1], but it is a perfectly well-defined quantity for general (nonequilibrium) systems, which are of central interest in this paper. The second term is a convolution integral and therefore Fourier transforming Eq. (47) leads to

$$\tilde{c}(\mathbf{k}) = \frac{\tilde{h}(\mathbf{k})}{1+\rho\tilde{h}(\mathbf{k})}, \tag{48}$$

where $\tilde{c}(\mathbf{k})$ is the Fourier transform of $c(\mathbf{r})$. Using relation (28) and definition (48), we can reexpress the number variance for a window of arbitrary shape in terms of the Fourier transform of the direct correlation function as follows:

$$\langle N^2(\mathbf{R})\rangle - \langle N(\mathbf{R})\rangle^2 = \langle N(\mathbf{R})\rangle\left[\frac{1}{(2\pi)^d}\int \frac{\tilde{\alpha}(\mathbf{k};\mathbf{R})}{1-\rho\tilde{c}(\mathbf{k})}d\mathbf{k}\right]. \tag{49}$$

We know that for a hyperuniform system, $\tilde{h}(0) = -1/\rho$ by definition, i.e., the volume integral of $h(\mathbf{r})$ exists and, in particular, $h(\mathbf{r})$ is a short-ranged function that decays to zero faster than $|\mathbf{r}|^{-d}$. Interestingly, this means that the denominator on the right-hand side of Eq. (48) vanishes at $\mathbf{k}=\mathbf{0}$ and therefore $\tilde{c}(\mathbf{k}=\mathbf{0})$ diverges to $-\infty$. This implies that the real-space direct correlation function $c(\mathbf{r})$ is long ranged, i.e., decays slower than $|\mathbf{r}|^{-d}$, and hence the volume integral of $c(\mathbf{r})$ does not exist. This is an unconventional behavior because, in most equilibrium instances, $c(\mathbf{r})$ is a short-ranged function, even in the vicinity of thermodynamic critical points where $h(\mathbf{r})$ is long ranged. One can see that $c(\mathbf{r})$ for a hyperuniform system behaves similarly to the total correlation function $h(\mathbf{r})$ for an equilibrium system near its critical point [19], i.e., each of these functions in these respective instances become long ranged. If this analogy holds, then one expects the direct correlation function for hyperuniform systems to have the following asymptotic behavior for large $r\equiv|\mathbf{r}|$ and sufficiently large d:

$$c(\mathbf{r}) \sim -\frac{1}{r^{d-2+\eta}} \quad (r\to\infty), \tag{50}$$

where $(2-d) < \eta \leqslant 2$ is a new "critical" exponent associated with $c(\mathbf{r})$ for hyperuniform systems that depends on the space dimension [25]. For noninteger values of η, the asymptotic relation (50) implies that the Fourier transform $\tilde{h}(\mathbf{k})$ is a nonanalytic function of $k\equiv|\mathbf{k}|$. We will show in Sec. V that there is a class of hyperuniform systems that obey Eq. (50) but with integer values of η, implying that $\tilde{h}(\mathbf{k})$ is an analytic function of k. Inversion of Eq. (50) yields

$$\tilde{c}(\mathbf{k}) \sim -\frac{1}{k^{2-\eta}} \quad (k\to 0), \tag{51}$$

which, when combined with Eq. (48), yields the asymptotic form of the structure factor

$$S(\mathbf{k}) \sim k^{2-\eta} \quad (k\to 0). \tag{52}$$

The specific asymptotic form of $S(\mathbf{k})$ for small k contributes to determining the "universality" class of the hyperuniform system.

Let us now consider a point pattern with a reduced density ϕ that is nearly hyperuniform and that can be made hyper-

TABLE I. Definitions of the critical exponents in the vicinity of or at the hyperuniform state. Here $S^{-1}(0)$ is the inverse of the structure factor at $k=0$, ξ is the correlation length, and $c(r)$ is the direct correlation function.

Exponent	Asymptotic behavior
γ	$S^{-1}(0)\sim\left(1-\frac{\phi}{\phi_c}\right)^{-\gamma}$ $(\phi\to\phi_c^-)$
γ'	$S^{-1}(0)\sim\left(\frac{\phi}{\phi_c}-1\right)^{-\gamma'}$ $(\phi\to\phi_c^+)$
ν	$\xi\sim\left(1-\frac{\phi}{\phi_c}\right)^{-\nu}$ $(\phi\to\phi_c^-)$
ν'	$\xi\sim\left(\frac{\phi}{\phi_c}-1\right)^{-\nu'}$ $(\phi\to\phi_c^+)$
η	$c(r)\sim r^{2-d-\eta}$ $(\phi=\phi_c)$

uniform by increasing and/or decreasing the density. We denote by ϕ_c the reduced density at the hyperuniform state. The reduced densities ϕ and ϕ_c play the same role as temperature T and critical temperature T_c, respectively, in the analogous thermal problem in the vicinity of a critical point. Thus, we can define critical exponents associated with the manner in which certain quantities diverge as the critical (hyperuniform) point is approached. For example, for $|\phi_c-\phi|\ll 1$, the inverse of the structure factor at $k=0$, $S^{-1}(0)$ and the *correlation length* ξ obey the power laws

$$S^{-1}(0)\sim\left(1-\frac{\phi}{\phi_c}\right)^{-\gamma},\quad \phi\to\phi_c^-, \tag{53}$$

$$\xi\sim\left(1-\frac{\phi}{\phi_c}\right)^{-\nu},\quad \phi\to\phi_c^-, \tag{54}$$

where γ and ν are non-negative critical exponents that are related by the formula

$$\gamma=(2-\eta)\nu. \tag{55}$$

As will be discussed in Sec. V, ξ characterizes the decay of the direct correlation function in the vicinity of $\phi=\phi_c$. Analogous critical exponents can be defined for densities near but above ϕ_c, as summarized in Table I. In Sec. V B, we determine the critical exponents exactly for certain models of disordered point patterns in d dimensions.

III. VARIANCE FORMULA FOR A SINGLE-POINT PATTERN

In this section, we derive a new formula for the number variance of a single realization of a point pattern consisting of a large number of points N in a large system of volume V. This is necessarily a volume-average formulation. Fluctuations for a fixed window size arise because we let the window uniformly sample the space. As we will show, depending on the nature of the point pattern, this formula will generally lead to a result that is different from formula (22), which was derived for a statistically homogeneous system. We also show that the formula derived here is preferable for finding point patterns with an extremal or targeted value of the number variance.

For notational simplicity, we consider a d-dimensional spherical window of radius R, keeping in mind that the results of this section apply as well (with obvious notational changes) to regular domains of arbitrary shape. We assume that the characteristic size of the system is much larger than the window radius so that boundary effects can be neglected and that the large numbers $N\gg 1$ and $V\gg 1$ are comparable such that $\rho\equiv N/V$ is a finite number density. Let us recall relation (20) for the number of points $N(\mathbf{x}_0;R)$ contained within a window at position $\mathbf{x}_0$ in a system of volume V in which there are N points. We let the window uniformly sample the space and define the average number of points within the window to be

$$\overline{N(R)}\equiv\frac{1}{V}\int\sum_{V i=1}^{N} w(|\mathbf{r}_i-\mathbf{x}_0|;R)d\mathbf{x}_0=\rho\int_V\Theta(R-r)d\mathbf{r}$$
$$=\rho v_1(R)=2^d\phi\left(\frac{R}{D}\right)^d, \tag{56}$$

where $v_1(r)$ and ϕ are given by Eqs. (33) and (34), respectively.

Similarly, squaring relation (20) and averaging yields

$$\overline{N^2(R)}=\frac{1}{V}\int\sum_{V i=1}^{N} w(|\mathbf{r}_i-\mathbf{x}_0|;R)d\mathbf{x}_0$$
$$+\frac{1}{V}\int\sum_{V i\neq j}^{N} w(|\mathbf{r}_i-\mathbf{x}_0|;R)w(|\mathbf{r}_j-\mathbf{x}_0|;R)d\mathbf{x}_0$$
$$=\rho v_1(R)+\frac{\rho v_1(R)}{N}\sum_{i\neq j}^{N}\alpha(r_{ij};R), \tag{57}$$

where $\alpha(r;R)$ is the scaled intersection volume, given explicitly by Eq. (A5), and $r_{ij}=|\mathbf{r}_i-\mathbf{r}_j|$. Therefore, the local variance $\sigma^2(R)$ is given by

$$\sigma^2(R)\equiv\overline{N^2(R)}-\overline{N(R)}^2$$
$$=\overline{N(R)}\left[1-\rho v_1(R)+\frac{1}{N}\sum_{i\neq j}^{N}\alpha(r_{ij};R)\right]$$
$$=2^d\phi\left(\frac{R}{D}\right)^d\left[1-2^d\phi\left(\frac{R}{D}\right)^d+\frac{1}{N}\sum_{i\neq j}^{N}\alpha(r_{ij};R)\right]. \tag{58}$$

The last term within the brackets is the sum of scaled intersection volumes between all point pairs, per point.

Remarks:

(1) It is important to observe that the series in Eq. (58) terminates for $r_{ij}>2R$ even for infinitely large systems.

(2) Note that the variance formula (58) is different from the ensemble-average formula (22), which involves an additional weighted average over pairs of points; thus, the ap-

pearance of the total correlation function $h(\mathbf{r})$. Therefore, the variance function (58), unlike the variance function (22), will generally contain small-scale fluctuations with respect to R, of wavelength on the order of the mean separation between the points that are superposed on the large-scale variations with respect to R (see examples in Sec. IV). Expressions (58) and (22) are identically the same for statistically homogeneous (infinite) systems, in which case the amplitudes of the small-scale fluctuations vanish.

(3) Because the variance formula is valid for a single realization, one can use it, in principle, to find the particular point pattern that minimizes the variance at a fixed value of R. In other words, it is desired to minimize $\sigma^2(R)$ for a particular value of R among all $r_{ij} \leqslant 2R$, i.e.,

$$\min_{\forall r_{ij} \leqslant 2R} \sigma^2(R), \tag{59}$$

where $\sigma^2(R)$ is given by Eq. (58). The scaled intersection volume $\alpha(r_{ij};R)$ appearing in Eq. (58) is a non-negative function of r_{ij} (see Fig. 9) and can be viewed as a *repulsive* pair potential between a point i and a point j. Finding the global minimum of $\sigma^2(R)$ is equivalent to determining the ground state for the "potential energy" function represented by the pairwise sum in Eq. (58). Such global optimization problems can be attacked using simulated annealing techniques, for example. More generally, one could devise an optimization scheme in which a *targeted* value of the variance (rather than an extremal value) is sought [26].

(4) Because the pairwise sum in Eq. (58) is positive, we immediately obtain from Eq. (58) the following lower bound on the variance:

$$\sigma^2(R) \geqslant 2^d \phi \left(\frac{R}{D}\right)^d \left[1 - 2^d \phi \left(\frac{R}{D}\right)^d\right]. \tag{60}$$

This bound is exact for $R \leqslant r_{\min}/2$, where $r_{\min}$ is the minimum pairwise distance, and therefore provides an accurate estimate of the variance for small R. For sufficiently large R, however, the bound becomes negative and therefore provides a poor estimate of the variance.

(5) For large R in the special case of hyperuniform systems, the large-scale variations in R will grow as R^{d-1}, and so we have from Eq. (58) that

$$\sigma^2(R) = \Lambda(R)\left(\frac{R}{D}\right)^{d-1} + O\left(\frac{R}{D}\right)^{d-2}, \tag{61}$$

where

$$\Lambda(R) = 2^d \phi \left(\frac{R}{D}\right)\left[1 - 2^d \phi \left(\frac{R}{D}\right)^d + \frac{1}{N}\sum_{i \neq j}^{N} \alpha(r_{ij};R)\right] \tag{62}$$

is the asymptotic "surface-area" function that contains the small-scale variations in R.

(6) It is useful to average the small-scale function $\Lambda(R)$ over R to yield the constant

$$\overline{\Lambda}(L) = \frac{1}{L}\int_0^L \Lambda(R)\, dR, \tag{63}$$

where $\Lambda(R)$ is given by Eq. (62). In the case of a statistically homogeneous system, the constant surface-area coefficient

$$\overline{\Lambda} \equiv \lim_{L \to \infty} (L) = \lim_{L \to \infty} \frac{1}{L}\int_0^L \Lambda(R)\, dR \tag{64}$$

is trivially related to the surface-area coefficient B, defined by Eq. (37) in the asymptotic ensemble-average formula, by the expression

$$\overline{\Lambda} = 2^d \phi B = \frac{-\ 2^{d-1}\phi^2 d\Gamma(d/2)}{D v_1(D/2)\Gamma\left(\frac{d+1}{2}\right)\Gamma\left(\frac{1}{2}\right)} \int_{\Re^d} h(\mathbf{r})\, r\, d\mathbf{r}. \tag{65}$$

(7) Because the formula for the coefficient $\overline{\Lambda}$ is defined for a single realization, we can employ it to obtain the particular point pattern that minimizes it. Thus, the optimization problem is the following:

$$\min_{\forall r_{ij} \leqslant 2L} \overline{\Lambda}, \tag{66}$$

where $\overline{\Lambda}$ is given by Eq. (63).

(8) For large systems in which any point "sees" an environment typical of all points, relation (58) for the variance can be simplified. This requirement is met by all infinite periodic lattices for any R as well as statistically homogeneous point patterns for sufficiently large R. In such instances, the second term within the brackets of Eq. (58) can be written as sum of scaled intersection volumes over $N-1$ points and some reference point. Thus, we can rewrite the variance as

$$\sigma^2(R) = 2^d \phi \left(\frac{R}{D}\right)^d \left[1 - 2^d \phi \left(\frac{R}{D}\right)^d + \sum_{k=1}^{N-1} \alpha(r_k;R)\right], \tag{67}$$

where r_k is the distance from the reference point to the kth point. The asymptotic expression (61) for $\sigma^2(R)$ and relation (63) for $\overline{\Lambda}(R)$ still apply but with $\Lambda(R)$ given by the simpler formula

$$\Lambda(R) = 2^d \phi \left(\frac{R}{D}\right)^d \left[1 - 2^d \phi \left(\frac{R}{D}\right)^d + \sum_{k=1}^{N-1} \alpha(r_k;R)\right]. \tag{68}$$

We emphasize that the simplified formulas (67) and (68) *cannot* be used for the aforementioned optimization calculations. The latter requires the full pairwise sum appearing in the general relation (58).

(9) In order to make the surface-area function $\Lambda(R)$ or surface-area coefficient $\overline{\Lambda}$ independent of the characteristic length scale or, equivalently, density of the hyperuniform point pattern, one can divide each of these quantities by $\phi^{(d-1)/d}$, i.e.,

$$\frac{\Lambda(R)}{\phi^{(d-1)/d}} \quad \text{or} \quad \frac{\overline{\Lambda}}{\phi^{(d-1)/d}}. \tag{69}$$

This scaling arises by recognizing that normalization of the asymptotic relation (61) by expression (56) for $\langle \bar{N}(R) \rangle$ taken to the power $(d-1)/d$ renders the resulting normalized relation independent of R/D. Such a scaling will be used to compare calculations of $\Lambda(R)$ and $\overline{\Lambda}$ for different ordered and disordered point patterns to one another in the subsequent sections. Note that since one-dimensional hyperuniform patterns have bounded fluctuations, this scaling is irrelevant for $d=1$.

IV. CALCULATIONS FOR INFINITE PERIODIC LATTICES

It is useful and instructive to compute the variance, using the formulas derived in the preceding section, for common infinite periodic lattices, which are hyperuniform systems. To our knowledge, explicit calculations have only been obtained for the square lattice [13] and triangular lattice [14] in two dimensions. Here we will obtain explicit results for other two-dimensional lattices as well as one- and three-dimensional lattices. We take the window to be a d-dimensional sphere of radius R.

For infinite periodic lattices, Fourier analysis leads to an alternative representation of the variance. Let the sites of the lattice be specified by the primitive lattice vector $\mathbf{P}$ defined by the expression

$$\mathbf{P} = n_1\mathbf{a}_1 + n_2\mathbf{a}_2 + \cdots + n_{d-1}\mathbf{a}_{d-1} + n_d\mathbf{a}_d, \tag{70}$$

where $\mathbf{a}_i$ are the basis vectors of the unit cell array and n_i spans all the integers for $i=1,2,\ldots,d$. Denote by U the unit cell and v_C its volume. It is clear that the number of points $N(\mathbf{x}_0;R)$ within the window at $\mathbf{x}_0$ [cf. Eq. (20)] in this instance becomes

$$N(\mathbf{x}_0;R) = \sum_{\mathbf{P}} \Theta(R - |\mathbf{P} - \mathbf{x}_0|), \tag{71}$$

where the sum is over all $\mathbf{P}$.

The number $N(\mathbf{x}_0;R)$ is a periodic function in the window position $\mathbf{x}_0$ and therefore it can be expanded in a Fourier series as

$$N(\mathbf{x}_0;R) = \rho v_1(R) + \sum_{\mathbf{q}\neq\mathbf{0}} a(\mathbf{q}) e^{i\mathbf{q}\cdot\mathbf{x}_0}, \tag{72}$$

where $\mathbf{q}$ is the reciprocal lattice vector such that $\mathbf{q}\cdot\mathbf{P} = 2\pi m$ (where $m = \pm 1, \pm 2, \pm 3, \ldots$) and the sum is over all $\mathbf{q}$ except $\mathbf{q}=\mathbf{0}$. Following Kendall and Rankin [14], the coefficients $a(\mathbf{q})$, for $\mathbf{q}\neq 0$, are given by

$$\begin{aligned} a(\mathbf{q}) &= \frac{1}{v_C}\int_U N(\mathbf{x}_0;R) e^{-i\mathbf{q}\cdot\mathbf{x}_0} d\mathbf{x}_0 \\ &= \frac{1}{v_C}\sum_{\mathbf{P}} \int_U \Theta(R - |\mathbf{P} - \mathbf{x}_0|) e^{-i\mathbf{q}\cdot\mathbf{x}_0} d\mathbf{x}_0 \\ &= \frac{1}{v_C}\int_{\Re^d} \Theta(R - |\mathbf{T}|) e^{i\mathbf{q}\cdot\mathbf{T}} d\mathbf{T} = \frac{1}{v_C}\left(\frac{2\pi}{qR}\right)^{d/2} R^d J_{d/2}(qR), \end{aligned} \tag{73}$$

where $J_\nu(x)$ is the Bessel function of order ν. Note that the integral in the third line is nothing more than the Fourier transform of the window indicator function, which is given by Eq. (A3). The analysis above assumes that there is one point per unit cell, i.e., we have considered Bravais lattices. One can easily generalize it to the case of an arbitrary number of points n_C per unit cell. Formula (73) would then involve $n_C - 1$ additional terms of similar form to the original one.

By Parseval's theorem for Fourier series, the number variance $\sigma^2(R)$ is given explicitly by

$$\begin{aligned} \sigma^2(R) &\equiv \frac{1}{v_C}\int_U [N(\mathbf{x}_0;R) - \rho v_1(R)]^2 d\mathbf{x}_0 \\ &= \sum_{\mathbf{q}\neq\mathbf{0}} a^2(\mathbf{q}) \\ &= \frac{R^d}{v_C^2}\sum_{\mathbf{q}\neq\mathbf{0}} \left(\frac{2\pi}{q}\right)^d [J_{d/2}(qR)]^2. \end{aligned} \tag{74}$$

One can easily obtain an asymptotic expression for the variance for large R by replacing the Bessel function in Eq. (74) by the first term of its asymptotic expansion, and thus we have

$$\sigma^2(R) = \Lambda(R)\left(\frac{R}{D}\right)^{d-1} + O\left(\frac{R}{D}\right)^{d-2}, \tag{75}$$

where D is a characteristic microscopic length scale, say, the lattice spacing, and

$$\Lambda(R) = \frac{2^{d+1}\pi^{d-1}D^{2d}}{v_C^2}\sum_{\mathbf{q}\neq\mathbf{0}} \frac{\cos^2[qR - (d+1)\pi/4]}{(qD)^{d+1}} \tag{76}$$

describes small-scale variations in R. As before, it is convenient to compute the average of $\Lambda(R)$ over R to give the surface-area coefficient:

$$\overline{\Lambda} = \lim_{L\to\infty}\frac{1}{L}\int_0^L \Lambda(R) dR = \frac{2^d\pi^{d-1}D^{2d}}{v_C^2}\sum_{\mathbf{q}\neq\mathbf{0}} \frac{1}{(qD)^{d+1}}. \tag{77}$$

It is useful here to apply the specialized volume-average formula (67) to the case of infinite periodic lattices. Recognizing that the configuration of an infinite periodic point pat-

tern may be characterized by the distances r_k and coordination numbers Z_k for the successive shells of neighbors ($k=1,2,3,\ldots$) from a lattice point, we find from Eq. (67) that the variance can also be represented as

$$\sigma^2(R)=2^d\phi\left(\frac{R}{D}\right)^d\left[1-2^d\phi\left(\frac{R}{D}\right)^d+\sum_{k=1}^{\infty}Z_k\alpha(r_k;R)\right]. \tag{78}$$

The asymptotic expression (61) for $\sigma^2(R)$ and relation (63) for the surface-area coefficient $\overline{\Lambda}(R)$ still apply but with $\Lambda(R)$ given by

$$\Lambda(R)=2^d\phi\left(\frac{R}{D}\right)\left[1-2^d\phi\left(\frac{R}{D}\right)^d+\sum_{k=1}^{\infty}Z_k\alpha(r_k;R)\right]. \tag{79}$$

Formula (78) was obtained by Kendall and Rankin [14] using a more complicated derivation. Moreover, their derivation only applies to periodic point patterns. Our more general formula (67) is also valid for statistically homogeneous point patterns. We also note that our most general volume-average representation (58) of the variance, from which formula (67) is derived, is applicable to arbitrary point patterns and its derivation is quite straightforward.

One can also evaluate the asymptotic coefficient $\overline{\Lambda}$ using the ensemble-average formula (65). Strictly speaking, this formula is not applicable to periodic point patterns because such systems are not statistically homogeneous (neither are they statistically isotropic). To see the potential problem that arises by naively applying Eq. (65), let the origin be a lattice point in the system and consider determining the radial distribution function $g_2(r)$ by counting the number of lattice points at a radial distance r_k from the origin. For a lattice in d dimensions, we have that

$$g_2(r)=\sum_{k=1}^{\infty}\frac{Z_k\delta(r-r_k)}{\rho s_1(r_k)}, \tag{80}$$

where $s_1(r)$ is the surface area of a sphere of radius r given by Eq. (14) and Z_k is the coordination number of the kth shell. It is seen that substitution of the corresponding total correlation function $h(r)\equiv g_2(r)-1$ into Eq. (65) results in a nonconvergent sum. However, using a convergence "trick" [27], one can properly assure a convergent expression by reinterpreting the surface-area coefficient (65) for a periodic lattice in the following manner:

$$\begin{aligned}\overline{\Lambda}&=\lim_{\beta\to 0^+}\frac{-2^{d-1}\phi^2 d\Gamma(d/2)}{Dv_1(D/2)\Gamma\left(\frac{d+1}{2}\right)\Gamma\left(\frac{1}{2}\right)}\int_{\Re^d}e^{-\beta r^2}h(r)r\,d\mathbf{r}\\&=\lim_{\beta\to 0^+}\frac{2^{d-1}\phi d}{D\Gamma\left(\frac{1}{2}\right)}\left[\frac{\phi\pi^{d/2}}{v_1(D/2)\beta^{(d+1)/2}}\right.\\&\quad\left.-\frac{\Gamma(d/2)}{\Gamma\left(\frac{d+1}{2}\right)}\sum_{k=1}^{\infty}Z_k r_k e^{-\beta r_k^2}\right].\end{aligned} \tag{81}$$

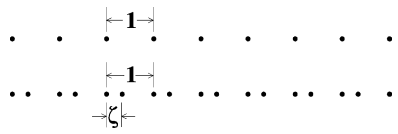

FIG. 3. Portions of two one-dimensional periodic point patterns, where $v_C=D=1$. The top and bottom arrays are the single-scale and two-scale examples, respectively.

A. One-dimensional examples

Here we obtain exact expressions for the number of points and number variance for general one-dimensional periodic point patterns using the aforementioned Fourier analysis. Using this result, we prove that the simple periodic linear array corresponds to the global minimum in $\overline{\Lambda}$. Subsequently, we employ the volume-average and ensemble-average formulations of Secs. II and III to obtain some of the same results in order to compare the three different methods. Recall that hyperuniform systems in one dimension have bounded fluctuations.

Let us first consider the simplest periodic point pattern in which each point is equi-distant from its near neighbors (see Fig. 3) and let this nearest-neighbor distance be unity ($v_C=D=1$). Applying relations (72) and (73) and recognizing that $\mathbf{q}=2\pi m\mathbf{a}_1/D$ ($m=\pm 1,\pm 2,\ldots$) for nonzero $\mathbf{q}$ yields the number of points contained within a one-dimensional window of radius R centered at position x_0:

$$N(R;x_0)=2R+\frac{2}{\pi}\sum_{m=1}^{\infty}\frac{\sin(2\pi mR)\cos(2\pi mx_0)}{m}. \tag{82}$$

According to relation (74), the associated variance is given by

$$\sigma^2(R)=\frac{2}{\pi^2}\sum_{m=1}^{\infty}\frac{\sin^2(2\pi mR)}{m^2}. \tag{83}$$

The variance $\sigma^2(R)$ is a periodic function with period 1/2 and is equal to the quadratic function $2R(1-2R)$ for $0\leqslant R\leqslant 1/2$ (see Fig. 4). Finally, the surface-area coefficient $\overline{\Lambda}$, defined by Eq. (77), which in one dimension amounts to the positional average of the variance for any value of R, is exactly given by the constant

$$\overline{\Lambda}=\frac{1}{\pi^2}\sum_{m=1}^{\infty}\frac{1}{m^2}=\frac{1}{6}. \tag{84}$$

It is known that this simple linear array yields the minimum value of $\overline{\Lambda}$ among all one-dimensional regular lattices. This is intuitively clear from the volume-average variance relation (58) for $d=1$; the linear repulsive effective "pair potential" contained therein is evidently responsible for such a minimum. However, heretofore it was not known whether this pattern corresponded to a global minimum, i.e., the smallest value of $\overline{\Lambda}$ among all infinite one-dimensional hyperuniform patterns. We now prove that the single-scale lat-

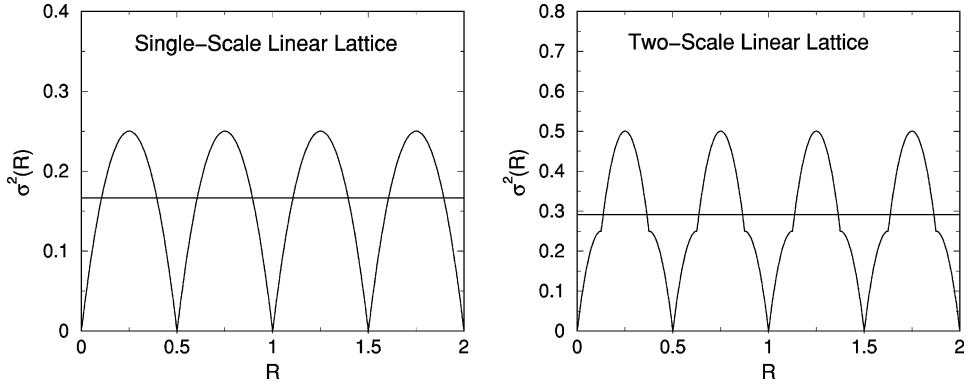

FIG. 4. Left panel: The quadratic periodic variance function $\sigma^2(R)$ for the single-scale periodic one-dimensional point pattern given by Eq. (83). The horizontal line is the average $\overline{\Lambda}=1/6$. Right panel: The piecewise-quadratic periodic variance function $\sigma^2(R)$ for the two-scale periodic one-dimensional point pattern given by Eq. (87) for the case $\zeta=1/4$. The horizontal line is the average $\overline{\Lambda}=7/24$.

tice indeed produces the global minimum. To prove this assertion, we utilize the identity

$$f(x)=\frac{1}{\pi^2}\sum_{m=1}^{\infty}\frac{1+2\cos(2\pi mx)}{m^2}=\frac{1}{2}-2x(1-x) \quad (85)$$

and note that $f(x)$ is a convex quadratic non-negative function for all real x. Now consider a case in which there are M points per unit cell in which the length of the unit cell is still unity. Thus, excluding the point at each lattice site, there are $M-1$ points inside the unit cell with positions $\zeta_1,\zeta_2,\ldots,\zeta_{M-1}$ such that each ζ_i lies in the interval (0,1). Without loss of generality, we arrange the $M-1$ points such that $\zeta_i<\zeta_{i+1}$ $(i=1,2,\ldots,M-2)$, *but their positions are otherwise arbitrary*. Following a similar analysis as the one above, we find that the number of points within a window centered at x_0 is exactly given by

$$N(R;x_0)=2MR+2\sum_{m=1}^{\infty}\frac{\sin(2\pi mR)\left\{\sum_{j=0}^{M-1}\cos[2\pi m(x_0-\zeta_j)]\right\}}{m}, \quad (86)$$

where $\zeta_0\equiv 0$. The variance is therefore given by

$$\sigma^2(R)=\frac{2}{\pi^2}\sum_{m=1}^{\infty}\frac{\sin^2(2\pi mR)\left\{M+\sum_{j=1}^{M-1}\cos(2\pi m\zeta_j)+\sum_{j<k}^{M-1}\cos[2\pi m(\zeta_k-\zeta_j)]\right\}}{m^2}. \quad (87)$$

We see that the variance $\sigma^2(R)$ for an arbitrary one-dimensional point pattern within the unit cell is a periodic function with period 1/2. (As we will see, the variance in higher dimensions is not a periodic function in R for periodic point patterns.) The average of the variance is exactly equal to the surface-area coefficient (77):

$$\overline{\Lambda}=\frac{1}{\pi^2}\sum_{m=1}^{\infty}\frac{M+\sum_{j=1}^{M-1}\cos(2\pi m\zeta_j)+\sum_{j<k}^{M-1}\cos[2\pi m(\zeta_k-\zeta_j)]}{m^2}=-\frac{M(M-3)}{12}+\sum_{j=1}^{M-1}f(\zeta_j)+\sum_{j<k}^{M-1}f(\zeta_k-\zeta_j), \quad (88)$$

where $f(x)$ is given by Eq. (85). Because $\overline{\Lambda}$ is given by a sum of convex quadratic non-negative functions, the global minimum is found from the zeros of the derivative $\partial\overline{\Lambda}/\partial\zeta_n$:

$$\frac{\partial\overline{\Lambda}}{\partial\zeta_n}=0=1-2\zeta_n+\sum_{j=1}^{n-1}(1-2\zeta_n+2\zeta_j)-\sum_{j=n+1}^{M-1}(1+2\zeta_n-2\zeta_j)$$
$$(n=1,2,\ldots,M-1). \quad (89)$$

It is easy to verify that the global minimum is achieved when the $M-1$ are uniformly distributed in the interval (0,1), i.e., $\zeta_n=n/M$ $(n=1,2,\ldots,M-1)$, yielding $\overline{\Lambda}=1/6$. Since this result is valid for arbitrary M, the simple single-scale lattice produces the global minimum value of $\overline{\Lambda}$ among all infinite one-dimensional hyperuniform point patterns.

Note that the single-scale lattice corresponds to the densest packing of one-dimensional congruent hard spheres (rods) on the real line. This might lead one to conjecture that the Bravais lattice associated with the densest packing of congruent spheres in any space dimension d provides the

TABLE II. The surface-area coefficient $\overline{\Lambda}$ for some ordered and disordered one-dimensional point patterns. The result for the two-scale lattice is for $\zeta \equiv \zeta_1 = 0.25$.

Pattern	ϕ	$\overline{\Lambda}$
Single-scale lattice	1	$1/6 \approx 0.166667$
Step+delta-function g_2	0.75	$3/16 = 0.1875$
Step-function g_2	0.5	$1/4 = 0.25$
Two-scale lattice	2	$7/24 \approx 0.291667$
Lattice gas	1	$1/3 \approx 0.333333$

minimal value of $\overline{\Lambda}$ among all periodic lattices for spherical windows. As we will see, this turns out to be the case for $d=2$, but not for $d=3$.

The variance as computed from Eq. (87) for the case $M=2$, which we call the "two-scale" lattice (see Fig. 3), is included in Fig. 4 for $\zeta \equiv \zeta_1 = 1/4$. In this instance, $\overline{\Lambda} = 7/24$. Clearly, the variance for the two-scale case bounds from above the variance for the single-scale case. Table II compares the surface-area coefficient for the single-scale and two-scale one-dimensional lattices. The other one-dimensional results summarized in Table II will be discussed in the ensuing sections. The potential use of the local variance as an order metric for hyperuniform point patterns in any dimension is discussed in Sec. VI.

Consider obtaining the volume-average representation of the variance for the two aforementioned one-dimensional periodic patterns from Eq. (78). Using relations (A5) and (A9) for the scaled intersection volume $\alpha(r;R)$, we find for any one-dimensional periodic point pattern in which $D=1$ that

$$\sigma^2(R) = 2\phi R\left[1 - 2\phi R + \sum_{k=1}^{M_R} Z_k\left(1 - \frac{r_k}{2R}\right)\Theta(2R - r_k)\right], \tag{90}$$

where M_R corresponds to the largest value of k for which $r_k < 2R$. Because in one dimension $\Lambda(R) = \sigma^2(R)$, where $\Lambda(R)$ is the function defined by Eq. (79), it follows that the average $\overline{\Lambda}$ is given by

$$\overline{\Lambda} = 2\int_0^{1/2} \Lambda(R)\,dR = \phi L\left[\left(1 - \frac{4\phi L}{3}\right) + \sum_{k=1}^{M_L} Z_k\left(1 - \frac{r_k}{2L}\right)^2\right], \tag{91}$$

where M_L corresponds to the largest value of k for which $r_k < 2L$. Using the fact that $\phi = 1$, $r_k = k$, and $Z_k = 2$ for all k for the single-scale lattice, one can easily reproduce the graph for $\sigma^2(R)$ depicted in Fig. 4 using relation (90) and verify that $\overline{\Lambda} = 1/6$ employing relation (91). Similarly, for the two-scale case, we have that $\phi = 2$, $r_k = k/4$, and $Z_k = 1$ for odd k, and $r_k = k/2$ and $Z_k = 2$ for even k. Hence, relation (90) leads to the same graph of the variance shown in Fig. 4, and relation (91) yields $\overline{\Lambda} = 7/24$ for $\zeta = 0.25$, as before.

We can also compute the surface-area coefficient using the ensemble-average relation (81). In one dimension, this relation yields

$$\overline{\Lambda} = \lim_{\beta \to 0^+}\left[\frac{\phi^2}{\beta} - \phi\sum_{k=1}^{\infty} Z_k r_k e^{-\beta r_k^2}\right], \tag{92}$$

where we have taken $D=1$. The sum in (92) can be evaluated exactly using the Euler-Maclaurin summation formula [28]. If $f(k)$ is a function defined on the integers, and continuous and differentiable in between, the Euler-Maclaurin summation formula provides an asymptotic expansion of the sum $\Sigma_{k=0}^{n} f(k)$ as $n \to \infty$. Applying this asymptotic formula to Eq. (92) in the cases of the single-scale and two-scale lattices yields that $\overline{\Lambda} = 1/6$ and $\overline{\Lambda} = 7/24$, respectively, which agree with the results obtained using the previous two methods. Although the Fourier-analysis and volume-average procedures are more direct methods to determine $\overline{\Lambda}$ for one-dimensional lattices, we will see that representation (81) provides an efficient means of computing $\overline{\Lambda}$ for lattices in higher dimensions.

B. Two-dimensional examples

Here we evaluate variance characteristics for the following four common two-dimensional lattices: square, triangular, honeycomb, and Kagomé lattices. From the lattice series (74), (76), and (77) with $d=2$, we have general two-dimensional series relations for the variance $\sigma^2(R)$, asymptotic surface-area function $\Lambda(R)$, and surface-area coefficient $\overline{\Lambda}$, respectively. For a specific lattice, the evaluation of any of these series requires the reciprocal lattice vector $\mathbf{q}$ and v_C. For example, for the square lattice, $\mathbf{q} = 2\pi(m_1\mathbf{a}_1 + m_2\mathbf{a}_2)/D$ $(m_i = 0, \pm 1, \pm 2, \ldots)$ for nonzero $\mathbf{q}$ and $v_C = D^2$. The sums are straightforward to evaluate, even if they converge slowly. Provided that R is not very large, however, the corresponding volume-average relations (78) and (79) are superior for computational purposes because the series involved are finite rather than infinite. For example, the asymptotic surface-area function $\Lambda(R)$ for the square lattice is plotted in Fig. 5 using Eq. (79) with Eq. (A10) for $1 \leqslant R \leqslant 4$. The function is seen to be aperiodic, but fluctuates around an average value in a bounded fashion. It is worth noting that the behavior of $\Lambda(R)$ for larger values of R is qualitatively the same. Interestingly, the average value of $\Lambda(R)$ over this small interval near $R=0$ (as well as other intervals of the same length) is quite close to the infinite-interval average value $\overline{\Lambda}$ [29].

The average value of the surface-area function $\Lambda(R)$ over all R, equal to the surface-area coefficient $\overline{\Lambda}$ [cf. Eq. (77)], is given (to six significant figures) by $\overline{\Lambda} = 0.457\,649$. Series (77) for the square lattice was first evaluated by Kendall [13]. Because it is a slowly converging series, he exploited certain results of number theory to reexpress the sum in terms of a more rapidly convergent series.

We found that numerical evaluation of the ensemble-average relation (81) is a simple and effective means of computing accurately the surface-area coefficient $\overline{\Lambda}$ for any common lattice. In two dimensions, this relation yields

$$\overline{\Lambda} = \lim_{\beta \to 0^+}\left[\frac{16\phi^2}{\pi^{1/2}\beta^{3/2}} - \frac{8\phi}{\pi}\sum_{k=1}^{\infty} Z_k r_k e^{-\beta r_k^2}\right]. \tag{93}$$

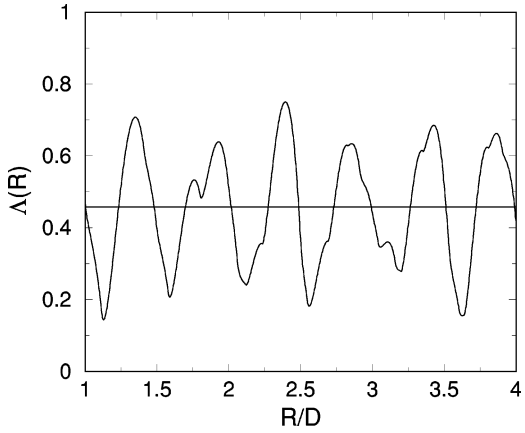

FIG. 5. The asymptotic surface-area function $\Lambda(R)$ for the square lattice for $1 \leqslant R \leqslant 4$, where D is the lattice spacing. The horizontal line is the asymptotic average value $\overline{\Lambda} = 0.457\,649$.

The sum in Eq. (93) is easily computed as a function of the convergence parameter β for any simple lattice. For sufficiently small β, this sum is linear in β and extrapolation to $\beta \to 0^+$ yields results that are accurate to at least six significant figures. We have also computed the surface-area coefficient for triangular, honeycomb, and Kagomé lattices. The result for the triangular lattice was first reported by Kendall and Rankin [14]. In Table III, we compare all of these results for the common two-dimensional lattices to one another by tabulating the normalized scale-independent surface-area coefficient, i.e., $\overline{\Lambda}/\phi^{1/2}$ [cf. Eq. (69)]. Rankin [30] proved that the triangular lattice has the smallest normalized surface-area coefficient for circular windows among all infinite periodic two-dimensional lattices, which is borne out in Table III. However, there is no proof that the triangular lattice minimizes $\overline{\Lambda}/\phi^{1/2}$ among all infinite two-dimensional hyperuniform point patterns for circular windows. Included in Table III are results for disordered point patterns that will be discussed in the ensuing sections.

Although the normalized surface-area coefficient is smallest for the triangular lattice, Table III reveals that the corresponding coefficients for the other lattices are not appreciably larger. This suggests that the fluctuating surface-area function $\Lambda(R)$ for nontriangular lattices may be smaller than the corresponding function for the triangular lattice for certain values of R. This is indeed the case as illustrated in Fig. 6, where the difference between the normalized scale-independent surface-area function $\Lambda(R)$ for the triangular and square lattices is plotted for the range $100D \leqslant R \leqslant 110D$ using relation (79). This difference oscillates rapidly about zero over this range of R, but the same qualitative trends occur for all values of R and for any pair of periodic lattices considered here. Given our previous interpretation of the global minimum of the variance as corresponding to the ground state of a many-particle system with a potential energy function given by $\alpha(r;R)$ (Sec. III), we see that the optimal lattice structure is sensitive to small changes in the value of R (which determines the range of the potential). This calls into question previous studies [31] that claim to have found stable ground-state lattices for two-dimensional systems of particles with purely repulsive interaction potentials of the same qualitative form as shown for $\alpha(r;R)$ in Fig. 9 with $d=2$.

C. Three-dimensional examples

Here we specialize to common infinite three-dimensional periodic lattices: simple cubic (sc) lattice, face-centered cubic (fcc) lattice, hexagonal-close-packed (hcp) lattice, body-centered cubic (bcc), and the diamond lattice. Explicit results for the number variance for such lattices have heretofore not been reported. From Eqs. (74), (76), and (77) with $d=3$, we have general three-dimensional relations for the variance $\sigma^2(R)$, asymptotic surface-area function $\Lambda(R)$, and surface-area coefficient $\overline{\Lambda}$, respectively. These expressions are easily evaluated for the specific lattice given v_C and the reciprocal lattice vectors $\mathbf{q}$. As we noted earlier, the volume-average relations (78) and (79) for $d=3$ are superior for computational purposes provided that R is not very large. Qualitatively, the three-dimensional trends for the surface-area function $\Lambda(R)$ are similar to the two-dimensional ones described above (see, for example, Figs. 5 and 6) and so we will not present explicitly such three-dimensional results here.

The ensemble-average relation (81), which for $d=3$ and $D=1$ yields

$$\overline{\Lambda} = \lim_{\beta \to 0^+} \left[\frac{72\phi^2}{\beta^2} - 6\phi \sum_{k=1} Z_k r_k e^{-\beta r_k^2} \right] \tag{94}$$

and provides an efficient means of computing the surface-area coefficient $\overline{\Lambda}$ for three-dimensional infinite periodic lat-

TABLE III. The surface-area coefficient $\overline{\Lambda}$ for some ordered and disordered two-dimensional point patterns. For ordered lattices, ϕ represents the close-packed covering fraction.

Pattern	ϕ	$\overline{\Lambda}/\phi^{1/2}$
Triangular lattice	$\pi/\sqrt{12} \approx 0.9069$	0.508347
Square lattice	$\pi/4 \approx 0.7854$	0.516401
Honeycomb lattice	$\pi/(3\sqrt{3}) \approx 0.6046$	0.567026
Kagomé lattice	$3\pi/(8\sqrt{3}) \approx 0.6802$	0.586990
Step+delta-function g_2	0.5	$2^{5/2}/(3\pi) \approx 0.600211$
Step-function g_2	0.25	$8/(3\pi) \approx 0.848826$
One-component plasma		$2/\sqrt{\pi} \approx 1.12838$

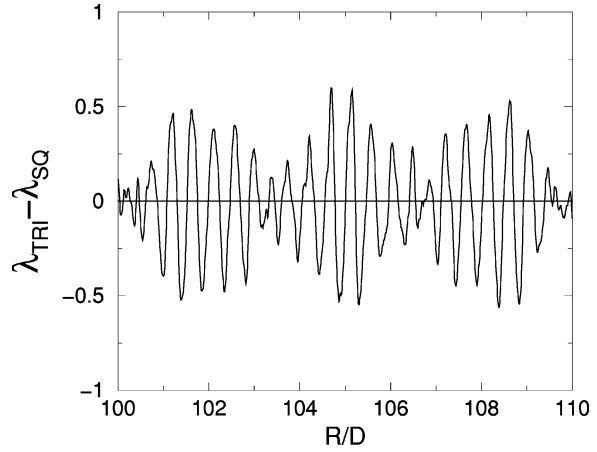

FIG. 6. The difference between the normalized scale-independent surface-area function $\Lambda(R)$ for the triangular and square lattices as a function of R, where D is the lattice spacing. Here $\lambda_{tri}=\Lambda(R)_{tri}/\phi_{tri}^{1/2}$ and $\lambda_{sq}=\Lambda(R)_{sq}/\phi_{sq}^{1/2}$.

tices by extrapolating the results for sufficiently small β to $\beta\to 0^+$. This has been carried out for all of the aforementioned common three-dimensional lattices and the results are summarized in Table IV, where we tabulate the normalized scale-independent surface-area coefficient, i.e., $\overline{\Lambda}/\phi^{2/3}$ [cf. Eq. (69)].

Contrary to the expectation $\overline{\Lambda}/\phi^{d/(d-1)}$ should, among all lattices, be a global minimum for the closest-packed lattices for spherical windows, we find that the minimum in three dimensions is achieved for the bcc lattice, albeit very close in numerical value to the fcc value (the next smallest value) [32]. This suggests that the closest-packed Bravais lattice for $d\geqslant 3$ does not minimize $\overline{\Lambda}/\phi^{d/(d-1)}$ [33]. Included in Table IV are results for disordered point patterns that will be discussed in the ensuing sections.

V. NONPERIODIC HYPERUNIFORM SYSTEMS

In this section, we briefly describe the known nonperiodic hyperuniform point patterns in one, two, and three dimensions and identify some others. For certain one-, two, and three- dimensional disordered hyperuniform point patterns, we exactly determine the corresponding surface-area coefficients, structure factors, direct correlation functions, and their associated critical exponents. A discussion concerning the potential use of surface-area coefficient $\overline{\Lambda}$ as an order metric for general hyperuniform point patterns is reserved for Sec. VI.

A. Examples

Statistically homogeneous hyperuniform point patterns in one dimension are not difficult to construct. Two examples are discussed here: one is a "lattice-gas" type model and the other is a construction due to Goldstein *et al.* [34]. The first example is constructed by tessellating the real line into regular intervals of length D. Then a single point is placed in each interval (independently of the others) at any real position with uniform random distribution. The number density $\rho=1/D$, and the pair correlation function is simply given by

$$g_2(r)=\begin{cases} r/D, & r\leqslant D \\ 1, & r>D. \end{cases} \tag{95}$$

One can easily verify that the system is hyperuniform ($A=0$) and that the surface-area coefficient (65) is given by

$$\overline{\Lambda}=\tfrac{1}{3}, \tag{96}$$

exactly twice the surface-area coefficient for the simple single-scale periodic point pattern [cf. Eq. (84)]. This one-dimensional lattice-gas model is a special case of the so-called d-dimensional shuffled lattice that we will describe below.

A less trivial example of a statistically homogeneous one-dimensional hyperuniform system is the construction of Goldstein *et al.* [34], which obtains from a homogeneous Poisson point process a new hyperuniform point process. This construction is defined as follows: First, one defines a statistically homogeneous process $X(x)$ on the real line such that $X(x)\leqslant 1$. This process is specified by dynamics such that $X(x)$ decreases at the rate of unity, except at the points of the Poisson process, where $X(x)$ jumps up by one unit unless this jump violates the upper bound condition, in which case no jump occurs. Second, one takes the points of the new point process to be those points in which $X(x)$ actually jumps. This new point process is hyperuniform. It is not known how to extend this construction to higher dimensions ($d\geqslant 2$).

TABLE IV. The surface-area coefficient $\overline{\Lambda}$ for some ordered and disordered three-dimensional point patterns. For ordered lattices, ϕ represents the close-packed covering fraction.

Pattern	ϕ	$\overline{\Lambda}/\phi^{2/3}$
bcc lattice	$3\pi/(8\sqrt{3})\approx 0.6802$	1.24476
fcc lattice	$\pi/\sqrt{18}\approx 0.7405$	1.24552
hcp lattice	$\pi/\sqrt{18}\approx 0.7405$	1.24569
sc lattice	$\pi/6\approx 0.5236$	1.28920
Diamond lattice	$3\pi/(16\sqrt{3})\approx 0.3801$	1.41892
Damped-oscillating g_2	0.46	1.44837
Step+delta-function g_2	0.3125	$5^{1/3}\times 9/2^{10/3}\approx 1.52686$
Step-function g_2	0.125	2.25

The construction of statistically homogeneous and isotropic point patterns that are hyperuniform in two or higher dimensions is a challenging task. An example of a statistically homogeneous d-dimensional system that is hyperuniform is the so-called *shuffled lattice* [35], but it is not statistically isotropic. This is a lattice whose sites are independently randomly displaced by a distance x in all directions according to some distribution with a finite second moment.

Gabrielli *et al.* [35] have observed that the a point pattern derived from the ''pinwheel'' tiling of the plane [36] has a number variance that grows as the surface area (perimeter) of the window, and is statistically homogeneous and isotropic. The prototile of the pinwheel tiling is a right triangle with sides of length 1, 2, and $\sqrt{5}$. The tiling is generated by performing certain ''decomposition'' and ''inflation'' operations on the prototile. In the first step, the prototile is subdivided into five copies of itself and then these new triangles are expanded to the size of the original triangle. These decomposition and inflation operations are repeated *ad infinitum* until the triangles completely cover the plane (see Fig. 7). It is obvious from the aforementioned discussion that the point pattern that results by randomly placing a point in each elementary triangle is hyperuniform. Importantly, because the tiles appear in *infinitely* many orientations, one can show that the resulting pattern is not only statistically homogeneous but also statistically isotropic. The full rotational invariance of the pattern is experimentally manifested by a diffraction pattern consisting of uniform rings rather than isolated Bragg peaks.

The one-component plasma is a statistical mechanical model that is known to have a number variance that grows only as the surface area of the window [17,37]. The one-component plasma is a system of point particles of charge e embedded in a uniform background that imparts overall charge neutrality. In $d=2$, the n-particle correlation functions for this model are exactly solvable in the thermodynamic limit when the coupling constant $\Gamma \equiv e^2/(kT)=2$ [38], and, in particular, the total correlation function is then given by

$$h(r)=-e^{-\pi\rho r^2}. \tag{97}$$

Substitution of Eq. (97) into Eq. (81) gives the surface area coefficient [37] as

$$\overline{\Lambda}=\frac{2}{\sqrt{\pi}}\phi^{1/2}, \tag{98}$$

where $\phi=\rho\pi D^2/4$. This evaluation of $\overline{\Lambda}$ is included in Table III. Observe that the structure factor of the d-dimensional one-component plasma at small k behaves as

$$S(k)\sim k^2 \quad (k\to 0) \tag{99}$$

and, therefore, the corresponding asymptotic behavior of the Fourier transform of the direct correlation function is given by

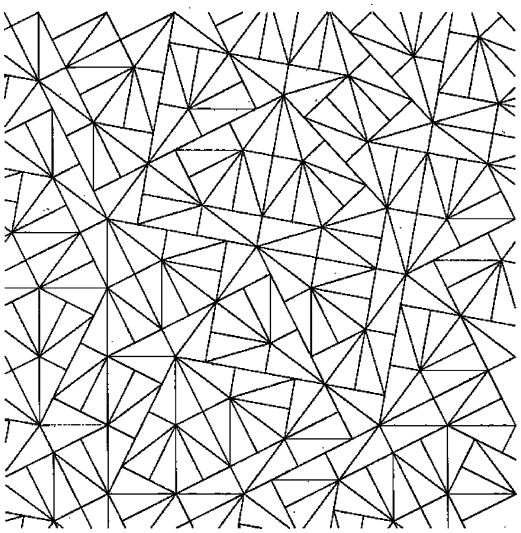

FIG. 7. Portion of a pinwheel tiling.

$$c(k)\sim -\frac{1}{k^2} \quad (k\to 0). \tag{100}$$

Another interesting model that is known to be hyperuniform [3,35] is the Harrison-Zeldovich [39] power spectrum for the primordial density fluctuations in the Universe. Here the structure factor for small k behaves as

$$S(k)\sim k. \tag{101}$$

Recently, Gabrielli *et al.* [35] have discussed the construction of point patterns in three dimensions that are consistent with the Harrison-Zeldovich spectrum.

The present authors have recently introduced and studied so-called g_2-invariant processes [20,40,41]. A g_2-invariant process is one in which a chosen non-negative form for the pair correlation function g_2 remains invariant over a nonvanishing density range while keeping all other relevant macroscopic variables fixed. The upper limiting ''terminal'' density is the point above which the non-negativity condition on the structure factor [cf. Eq. (18)] would be violated. Thus, at the terminal or critical density, the system is hyperuniform if realizable. In the following section, we will calculate the surface-area coefficient exactly for several of these g_2-invariant processes. We will also exactly determine the corresponding structure factors, direct correlation functions, and their associated critical exponents.

Interestingly, random packings of spheres near the maximally random jammed (MRJ) state [42,43] appear to be hyperuniform. Figure 8 depicts that the structure factor for such a computer-generated 40 000-particle packing is vanishingly small for small wave numbers. The packing is strictly jammed [44], which means that the particle system remains mechanically rigid under attempted global deformations (including shear) that do not increase volume and, furthermore, the packing is saturated. A *saturated* packing of hard spheres is one in which there is no space available to add another sphere. In the case of saturated packings of identical hard spheres of unit diameter, no point in space has distance

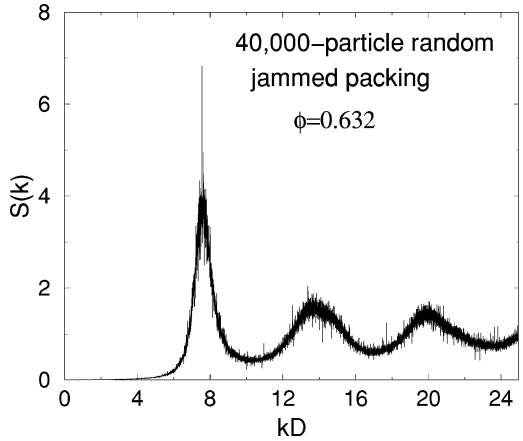

FIG. 8. The structure factor for a random packing of three-dimensional identical hard spheres of diameter D near the MRJ state [42,43] as computed from a single realization consisting of 40 000 particles in a cubical box with periodic boundary conditions using the protocol described in Ref. [43]. The packing (covering) fraction of spheres ϕ is 0.632.

greater than unity from the center of some sphere. An interesting postulate would be that all strictly jammed saturated infinite packings of identical spheres are hyperuniform. Examples of strictly jammed saturated periodic packings in two and three dimensions include the closest-packed triangular and face-centered cubic lattices, respectively. In light of this discussion, one can view a disordered packing near the MRJ state as a type of "glass" for the hard-sphere system. An important open fundamental question is whether there are molecular glasses (with "soft" intermolecular potentials) that become hyperuniform in the limit at which the temperature vanishes. Indeed, our preliminary results indicate that this possibility is attainable.

B. Exact results for g_2-invariant processes

Here we evaluate the surface-area coefficient exactly for three different disordered g_2-invariant processes studied by us earlier [20,40,41]. We also exactly determine the corresponding structure factors, direct correlation functions, and their associated critical exponents.

1. Step function g_2

Let us first consider the g_2-invariant process in which a spherically symmetric pair correlation or radial distribution function is defined by the unit step function [40]:

$$g_2(r)=\Theta(r-D)=\begin{cases}0, & r\leqslant D\\ 1, & r>D.\end{cases} \tag{102}$$

The condition $g_2(r)=0$ for $r\leqslant D$ prevents any pair of points from getting closer than a distance D to one another. Note that in the special case of a system of identical hard spheres in equilibrium in the limit $\rho\to 0$, g_2 is exactly given by Eq. (102). The corresponding total correlation function is given by

$$h(r)=-\Theta(D-r)=\begin{cases}-1, & r\leqslant D\\ 0, & r>D,\end{cases} \tag{103}$$

which when substituted into Eqs. (43) and (44) yields the volume and surface-area coefficients as

$$A=S(k=0)=1-2^d\phi,\quad B=\frac{\overline{\Lambda}}{2^d\phi}=\frac{2^{d-2}d^2\Gamma(d/2)}{\Gamma[(d+3)/2]\Gamma(1/2)}\phi. \tag{104}$$

The reduced density ϕ defined by Eq. (34) (equivalent to the covering fraction of the hard cores of diameter D) lies in the range $0\leqslant\phi\leqslant\phi_c$, where

$$\phi_c=\frac{1}{2^d} \tag{105}$$

is the terminal or critical density, i.e., the density at which the system is hyperuniform, where $A=0$ and

$$B=\overline{\Lambda}=\frac{d^2\Gamma(d/2)}{4\Gamma[(d+3)/2]\Gamma(1/2)}. \tag{106}$$

The values of the scale-independent surface-area coefficient $\overline{\Lambda}/\phi^{(d-1)/d}$ for $d=1,2$, and 3 are given in Tables II, III, and IV, respectively. It is worth noting that a recent study [45] provides convincing numerical evidence that the step-function g_2 is realizable by systems of impenetrable d-dimensional spheres (with $d=1$ and $d=2$) for densities up to the terminal density. Thus, it appears that satisfying the non-negativity conditions on $g_2(r)$ and $S(k)$ in this instance is sufficient to ensure realizability.

The Fourier transform of the total correlation function (103) yields the analytic function

$$\tilde{h}(k)=-\left(\frac{2\pi}{kD}\right)^{d/2}D^dJ_{d/2}(kD). \tag{107}$$

Thus, use of Eq. (15) gives the structure factor for ϕ in the range $0\leqslant\phi\leqslant\phi_c$ to be

$$S(k)=1-\Gamma(1+d/2)\left(\frac{2}{kD}\right)^{d/2}\left(\frac{\phi}{\phi_c}\right)J_{d/2}(kD). \tag{108}$$

Similarly, the Ornstein-Zernike relation (48) yields an exact expression for the Fourier transform of the direct correlation function:

$$\tilde{c}(k)=\frac{-\left(\frac{2\pi}{kD}\right)^{d/2}D^dJ_{d/2}(kD)}{1-\Gamma(1+d/2)\left(\frac{2}{kD}\right)^{d/2}\left(\frac{\phi}{\phi_c}\right)J_{d/2}(kD)}. \tag{109}$$

Thus, the small-k expansions of $S(k)$ and $\tilde{c}(k)$, which determine their behavior in the vicinity of, and at, the critical point, are, respectively, given by

$$S(k)=\left(1-\frac{\phi}{\phi_c}\right)+\frac{1}{2(d+2)}\frac{\phi}{\phi_c}(kD)^2+O((kD)^4) \tag{110}$$

and

$$\tilde{c}(k)=\frac{-v_1(D)}{\left(1-\frac{\phi}{\phi_c}\right)+\frac{1}{2(d+2)}\frac{\phi}{\phi_c}(kD)^2+O((kD)^4)}, \tag{111}$$

where $v_1(D)$ is the volume of a d-dimensional sphere of radius D [cf. Eq. (33)]. At the critical point $\phi=\phi_c$, we see that $S(k)\sim k^2$ and $\tilde{c}(k)\sim -k^{-2}$, and therefore comparison to Eqs. (52) and (51) yields the exponent $\eta=0$. Relation (110) leads to the power law

$$S^{-1}(0)=\left(1-\frac{\phi}{\phi_c}\right)^{-1}, \quad \phi\to\phi_c^-, \tag{112}$$

which upon comparison to Eq. (53) immediately yields the critical exponent $\gamma=1$. The correlation length ξ is defined via Eq. (111), which we rewrite as

$$k^2\tilde{c}(k)+\xi^{-2}\tilde{c}(k)=-G, \quad kD\ll 1, \tag{113}$$

where

$$\xi=\frac{D}{[2(d+2)\phi_c]^{1/2}}\left(1-\frac{\phi}{\phi_c}\right)^{-1/2}, \quad \phi\to\phi_c^-, \tag{114}$$

$$G=\frac{2(d+2)v_1(D)}{D^2}\frac{\phi_c}{\phi}, \tag{115}$$

and $v_1(D)$ is the volume of a sphere of radius D defined by Eq. (33). Comparison of Eq. (114) to the power law (54) yields the exponent $\nu=1/2$. Note that the exponent values $\gamma=1$, $\xi=1/2$, and $\eta=0$ are consistent with interrelation (55). Inversion of Eq. (113) yields the partial differential equation

$$\nabla^2 c(r)-\xi^{-2}c(r)=G\delta(\mathbf{r}), \quad r\gg D, \tag{116}$$

where the spherically symmetric Laplacian operator ∇^2 in any dimension d is given by

$$\nabla^2=\frac{1}{r^{d-1}}\frac{\partial}{\partial r}\left[r^{d-1}\frac{\partial}{\partial r}\right]. \tag{117}$$

We see that the direct correlation function in real space for large r is determined by Green's function of the linearized Poisson-Boltzmann equation.

Let us first determine the solutions of Eq. (116) at the critical point $\phi=\phi_c$ where ξ diverges to infinity. Thus, the asymptotic behavior of $c(r)$ for $r\gg D$ is given by the infinite-space Green's function for the d-dimensional Laplace equation [42], and so we obtain

$$c(r)=\begin{cases}-6\left(\frac{r}{D}\right), & d=1\\ 4\ln\left(\frac{r}{D}\right), & d=2\\ -\frac{2(d+2)}{d(d-2)}\left(\frac{r}{D}\right)^{d-2}, & d\geqslant 3.\end{cases} \tag{118}$$

Observe that it is only for $d\geqslant 3$ that $c(r)$ follows the power-law form (51) with an exponent $\eta=0$. The fact that η takes an integer value is due to the fact that $\tilde{h}(k)$ is an analytic function. Note also that the real-space direct correlation function of the one-component plasma has precisely the same asymptotic form as Eq. (118), albeit with different amplitudes (prefactors).

As $\xi\to\infty$ for fixed r, the solutions of Eq. (116) are

$$c(r)=\begin{cases}-6\frac{\phi_c}{\phi}\left(\frac{\xi}{D}\right)\exp(-r/\xi), & d=1\\ 4\frac{\phi_c}{\phi}\ln\left(\frac{r}{D}\right)\exp(-r/\xi), & d=2\\ -\frac{2(d+2)\phi_c}{d(d-2)\phi}\left(\frac{r}{D}\right)^{d-2}\exp(-r/\xi), & d\geqslant 3.\end{cases} \tag{119}$$

On the other hand, it is worth noting that as $r\to\infty$ for fixed ξ, the asymptotic behavior changes according to the relation

$$c(r)=-\frac{(d+2)\sqrt{2\pi}\phi_c}{\Gamma(1+d/2)\phi}\left(\frac{D}{\xi}\right)^{(d-3)/2}\left(\frac{D}{r}\right)^{(d-1)/2}\times\exp(-r/\xi), \quad d\geqslant 1. \tag{120}$$

2. Step+delta function g_2

Here we consider the g_2-invariant process defined by a radial distribution function that consists of the aforementioned unit step function plus a δ function contribution that acts at $r=D$:

$$g_2(r)=\Theta(r-D)+\frac{Z}{\rho s_1(D)}\delta(r-D), \tag{121}$$

where Z is a non-negative constant and $s_1(D)$ is the surface area of a sphere of radius D defined by Eq. (14). Function (121) was one of several examples studied by Torquato and Stillinger [20] to understand the relationship between short-range order and maximal density in sphere packings. In this investigation, Z was interpreted as the average contact coordination number. Here we consider their case IV (given in the appendix of Ref. [20]) in which the condition

$$Z=\frac{2^d d}{d+2}\phi \tag{122}$$

is obeyed in order to constrain the location of the minimum of the structure factor to be at $k=0$. Here the reduced density ϕ lies in the range $0\leqslant\phi\leqslant\phi_c$, and

$$\phi_c = \frac{d+2}{2^{d+1}} \tag{123}$$

is the terminal or critical density. Note that the function specified by relation (121) is a special limit of the radial distribution function corresponding to the dilute and narrow limit of the square-well potential studied by Sakai, Stillinger, and Torquato [41].

Substitution of Eq. (121) into Eqs. (43) and (44) yields the volume and surface-area coefficients as

$$A = S(k=0) = 1 - \frac{2^{d+1}}{d+2}\phi,$$

$$B = \frac{\overline{\Lambda}}{2^d \phi} = \frac{2^{d-2} d^2 \Gamma(d/2)}{(d+2)\Gamma((d+3)/2)\Gamma(1/2)}\phi. \tag{124}$$

At the critical density, $A=0$ and

$$\overline{\Lambda} = 2^d \phi_c B = \frac{d^2(d+2)\Gamma(d/2)}{16\Gamma[(d+3)/2]\Gamma(1/2)}. \tag{125}$$

The values of the scale-independent surface-area coefficient $\overline{\Lambda}/\phi^{(d-1)/d}$ for $d=1$,2 and 3 are given in Tables II, III, and IV, respectively.

The combination of relations (15), (48), and (121) gives the structure factor and Fourier transform of the direct correlation function, respectively, for ϕ in the range $0 \leqslant \phi \leqslant \phi_c$:

$$S(k) = 1 + \frac{2^{d/2}\Gamma(2+d/2)}{(kD)^{(d/2)-1}}\left(\frac{\phi}{\phi_c}\right)\left[\frac{J_{(d/2)-1}(kD)}{d+2} - \frac{J_{d/2}(kD)}{kD}\right], \tag{126}$$

$$\tilde{c}(k) = \frac{\dfrac{(2\pi)^{d/2} D^d}{(kD)^{(d/2)-1}}\left[\dfrac{J_{(d/2)-1}(kD)}{d+2} - \dfrac{J_{d/2}(kD)}{kD}\right]}{1 + \dfrac{2^{d/2}\Gamma(2+d/2)}{(kD)^{(d/2)-1}}\left(\dfrac{\phi}{\phi_c}\right)\left[\dfrac{J_{(d/2)-1}(kD)}{d+2} - \dfrac{J_{d/2}(kD)}{kD}\right]}. \tag{127}$$

Therefore, the Taylor expansions of $S(k)$ and $\tilde{c}(k)$ about $k=0$ are, respectively, given by

$$S(k) = \left(1 - \frac{\phi}{\phi_c}\right) + \frac{1}{8(d+2)(d+4)}\frac{\phi}{\phi_c}(kD)^4 + O((kD)^6) \tag{128}$$

and

$$\tilde{c}(k) = \frac{-2v_1(D)}{\left(1 - \dfrac{\phi}{\phi_c}\right) + \dfrac{1}{8(d+2)(d+4)}\dfrac{\phi}{\phi_c}(kD)^4 + O[(kD)^6]}. \tag{129}$$

Relation (128) leads to the power law

$$S^{-1}(0) = \left(1 - \frac{\phi}{\phi_c}\right)^{-1}, \quad \phi \to \phi_c^-, \tag{130}$$

which upon comparison to Eq. (53) again yields the critical exponent $\gamma=1$. The correlation length ξ is defined via Eq. (129), which we rewrite as

$$k^4\tilde{c}(k) + \xi^{-4}\tilde{c}(k) = -G, \quad kD \ll 1, \tag{131}$$

where

$$\xi = \frac{D}{[8(d+2)(d+4)\phi_c]^{1/4}}\left(1 - \frac{\phi}{\phi_c}\right)^{-1/4}, \quad \phi \to \phi_c^-, \tag{132}$$

$$G = \frac{16(d+2)(d+4)v_1(D)}{D^4}\frac{\phi_c}{\phi}. \tag{133}$$

Comparison of Eq. (132) to the power law (54) yields the exponent $\nu=1/4$. We see that the exponent values $\gamma=1$, $\xi=1/4$, and $\eta=-2$ are consistent with inter-relation (55). Inversion of Eq. (131) yields the partial differential equation

$$\nabla^4 c(r) + \xi^{-4} c(r) = -G\,\delta(\mathbf{r}), \quad r \gg D, \tag{134}$$

where $\nabla^4 \equiv \nabla^2\nabla^2$ is the spherically symmetric biharmonic operator, and ∇^2 is given by Eq. (117).

The solutions of Eq. (134) at the critical point $\phi=\phi_c$ ($\xi \to \infty$) are given by the infinite-space Green's function for the d-dimensional biharmonic equation. It is only for $d \geqslant 5$ that the solutions admit a power law of form (54) with an exponent $\eta=-2$, namely,

$$c(r) = -\frac{8(d+2)(d+4)}{d(d-2)(d-4)}\left(\frac{D}{r}\right)^{d-4}, \quad d \geqslant 5. \tag{135}$$

3. Damped-oscillating g_2

In three dimensions, Torquato and Stillinger [20] also considered a g_2-invariant process that appends a damped-oscillating contribution to the aforementioned step+delta-function g_2. Specifically, they examined the radial distribution function

$$g_2(r) = \Theta(r-D) + \frac{Z}{\rho 4\pi D^2}\delta(r-D) + \frac{a_1}{r}e^{-a_2 r} \times \sin(a_3 r + a_4)\Theta(r-D). \tag{136}$$

Here we consider their case II, where at the terminal density $\phi_c=0.46$, $Z=2.3964$, $a_1=1.15$, $a_2=0.510$, $a_3=5.90$, and $a_4=1.66$. At this critical point, the volume coefficient $A=0$ and the surface-area coefficient (65) is given by

$$\overline{\Lambda} = 36\phi_c^2 - 6\phi_c Z + 144 a_1 \phi_c^2 I, \tag{137}$$

where

$$I=\int_1^\infty x e^{-a_2 x}\sin(a_3 x+a_4)dx=\frac{(2a_3^3-a_3^5-6a_2^2a_3-2a_2^2a_3^3-4a_2^3a_3-4a_2a_3^3-a_2^4a_3)}{(a_2^2+a_3^2)^3}e^{-a_2}\cos(a_3+a_4)$$
$$+\frac{(2a_3^4+6a_2a_3^2-a_2^5-2a_2^4-2a_2^3-a_2a_3^4-2a_2^3a_3^2)}{(a_2^2+a_3^2)^3}e^{-a_2}\sin(a_3+a_4).$$

Substitution of the aforementioned parameters in Eq. (137) yields $\overline{\Lambda}=0.863\,082$. This evaluation of $\overline{\Lambda}$ is included in Table IV. With this choice of g_2, the first nonzero term of the small-k expansion of the structure factor $S(k)$ at the critical point is of order k^4, and therefore the exponent $\eta=-2$, as in the previous case. However, here $c(r)$ does not admit the power-law form (50) for large r because $\eta<-1$.

VI. DISCUSSION AND CONCLUSIONS

The principal theme presented in this paper is that number fluctuations calculated for variable window geometries offer a powerful tool to characterize and to classify point-particle media. This theme encompasses both spatially periodic (crystalline) particle patterns and those that are globally disordered (amorphous). By considering the large-window asymptotic limit, special attention attaches to volume and to surface fluctuations in space dimension $d\geqslant 1$. A special class of "hyperuniform" point patterns has been recognized for which the volume fluctuations vanish identically; equivalently these are systems for which the structure factor $S(k)$ vanishes at $k=0$. Another special class of "hyposurficial" point patterns has also been recognized for which the surface fluctuations vanish identically. The first of these special attributes requires that the $(d-1)$-st spatial moment of the total correlation function be constrained in magnitude; the second requires a similar constraint on the dth spatial moment of the total correlation function. The preceding text demonstrates that no point pattern can simultaneously be both hyperuniform and hyposurficial.

All infinitely extended perfectly periodic structures are hyperuniform. We have stressed that geometrically less regular cases of hyperuniformity also exist, including those that are spatially uniform and isotropic. The suitably normalized surface fluctuation quantity, which measures the extent to which hyperuniform systems fail to attain hyposurficial status, becomes a natural non-negative order metric that we have evaluated numerically for a basic sampling of structures. We proved that the simple periodic linear array yields the global minimum value for hyperuniform patterns in $d=1$, and showed that the triangular lattice produces the smallest values for the cases tested in $d=2$. But in spite of the fact that these minimizing structures correspond to optimal packings of rods and disks, respectively, the face-centered-cubic lattice for optimal sphere packing does not minimize the surface-fluctuation order metric for $d=3$. Instead, the body-centered cubic lattice enjoys this distinction [46]. For each choice of space dimension, other lattices and irregular hyperuniform patterns yield higher values for this order metric. An order metric for hyperuniform systems based on the local variance may find potential use in categorizing "jammed" and "saturated" sphere packings [42–44,47] whose long-wavelength density fluctuations vanish.

It is clearly desirable to extend the set of point patterns for which the surface fluctuation order metric has been numerically evaluated. This would help to strengthen the impression created thus far that regardless of space dimension d, point patterns arranged by increasing values of the order metric are indeed essentially arranged by increasing structural disorder. It will be important in the future to include a selection of two- and three-dimensional quasicrystalline point patterns [48] in the comparisons; the presumption at the present state of understanding is that they would present order metrics with values that lie between the low magnitudes of periodic lattices, and the substantially larger magnitudes of spatially uniform, isotropic, irregular point patterns. It would also benefit insight to include cases of spatially uniform, but anisotropic, point patterns; for example, those associated with "hexatic" order in two dimensions [49].

An important class of hyperuniform systems arises from the so-called "g_2-invariant processes" [20,40,41,46]. These processes require that the pair correlation function $g_2(r)$ remain unchanged as density increases from zero. For those g_2-invariant processes that correspond to thermal equilibrium, this criterion is implemented by virtue of compensating continuous changes in the particle pair potential function. For any given choice of the invariant g_2, such a process is in fact achievable, but only for densities up to a terminal density limit. At this upper limit, the system of points attains hyperuniformity, i.e., $S(k)=0$. Furthermore, examination of the Ornstein-Zernike relation reveals that the direct correlation function $c(r)$ develops a long-range tail as the terminal density is approached from below. By implication, for the special case of a thermal equilibrium process, the pair potential at the terminal density develops a long-range repulsive Coulombic form. The conclusion is that hyperuniformity at that terminal density is logically associated with the local electroneutrality condition that all equilibrium systems of electrostatically charged particles must obey [50].

The Ornstein-Zernike relation, though originally conceived to apply to systems in thermal equilibrium, can nevertheless be formally applied to any system for which the pair correlation function $g_2(r)$ is available. Hyperuniform systems that are irregular and isotropic possess short-range pair correlation only, but as in the examples just cited the corresponding direct correlation functions are long ranged. In an important sense, hyperuniform systems exhibit a kind of "inverted critical phenomenon." For conventional liquid-

vapor critical points, $h(r) \equiv g_2(r) - 1$ is long ranged and implies diverging density fluctuations and isothermal compressibilities, while the direct correlation function $c(r)$ remains short ranged. Hyperuniform systems have short range for $h(r)$, vanishing volume fluctuations and isothermal compressibility, and a long-ranged $c(r)$.

As a final matter, we mention that an attractive direction for future study of hyperuniformity and related concepts involves consideration of collective density variables. These are defined by a nonlinear transformation of point-particle positions $\mathbf{r}_j$ $(1 \leqslant j \leqslant N)$ as follows:

$$\rho(\mathbf{k}) = \sum_{j=1}^{N} \exp(i\mathbf{k}\cdot\mathbf{r}_j). \tag{138}$$

If the particles interact through a spherically symmetric pair potential whose Fourier transform exists and is denoted by $V(k)$, then the overall potential energy for the N particles in volume V can be expressed in the following manner:

$$\Phi = \frac{1}{2V} \sum_{\mathbf{k}} V(k)[\rho(\mathbf{k})\rho(-\mathbf{k}) - N]. \tag{139}$$

It has been demonstrated [51] that at least in one dimension, application of a suitable $V(k)$, followed by Φ minimization, can totally suppress density fluctuations for $\mathbf{k}$'s near the origin. This automatically produces a hyperuniform system configuration. Analogous studies need to be pursued for two- and three-dimensional systems.

ACKNOWLEDGMENTS

We are grateful to Joel Lebowitz for bringing to our attention the problem of surface fluctuations and for many insightful discussions. We thank Aleksandar Donev, Andrea Gabrielli, Hajime Sakai, and Peter Sarnak for very helpful comments. This work was supported by the Petroleum Research Fund as administered by the American Chemical Society, by an MRSEC Grant at Princeton University, NSF Grant No. DMR-0213706, and by the Division of Mathematical Sciences at NSF under Grant No. DMS-0312067.

APPENDIX A: INTERSECTION VOLUME OF TWO IDENTICAL d-DIMENSIONAL SPHERES

In this appendix, we obtain an explicit expression for the scaled intersection volume of two identical d-dimensional spheres of radius R whose centers are separated by a distance r. This function $\alpha(r;R)$ is defined by Eq. (23).

We begin by noting that the d-dimensional Fourier transform (16) of any integrable function $f(r)$ that depends only on the modulus $r = |\mathbf{r}|$ of the vector $\mathbf{r}$ is given by [22]

$$\tilde{f}(k) = (2\pi)^{d/2} \int_0^\infty r^{d-1} f(r) \frac{J_{(d/2)-1}(kr)}{(kr)^{(d/2)-1}} dr, \tag{A1}$$

and the inverse transform (17) of $f(k)$ is given by

$$f(r) = \frac{1}{(2\pi)^{d/2}} \int_0^\infty k^{d-1} f(k) \frac{J_{(d/2)-1}(kr)}{(kr)^{(d/2)-1}} dk. \tag{A2}$$

Here k is the modulus of the wave vector $\mathbf{k}$ and $J_\nu(x)$ is the Bessel function of order ν.

The Fourier transform of the window indicator function (31) is given by

$$\begin{aligned}\tilde{w}(k;R) &= \frac{(2\pi)^{d/2}}{k^{(d/2)-1}} \int_0^R r^{d/2} J_{(d/2)-1}(kr) dr \\ &= \left(\frac{2\pi}{kR}\right)^{d/2} R^d J_{d/2}(kR).\end{aligned} \tag{A3}$$

Therefore, the Fourier transform of $\alpha(r;R)$, defined by Eq. (26), is given by

$$\tilde{\alpha}(k;R) = 2^d \pi^{d/2} \Gamma(1 + d/2) \frac{[J_{d/2}(kR)]^2}{k^d}. \tag{A4}$$

Using the inverse transform (A2) yields the scaled intersection volume function to be

$$\begin{aligned}\alpha(r;R) &= \frac{2^d \Gamma(1+d/2)}{r^{(d-2)/2}} \int_0^\infty \frac{[J_{d/2}(kR)]^2 J_{(d/2)-1}(kr) dk}{k^{d/2}} \\ &= I_{1-x^2}\left(\frac{d+1}{2}, \frac{1}{2}\right) \Theta(2R - r),\end{aligned} \tag{A5}$$

where

$$I_x(a,b) = \frac{B_x(a,b)}{B(a,b)} \tag{A6}$$

is the *normalized* incomplete beta function [28],

$$B_x(a,b) = \int_0^x t^{a-1}(1-t)^{b-1} dt, \tag{A7}$$

is the incomplete beta function, and

$$B(a,b) = \int_0^1 t^{a-1}(1-t)^{b-1} dt = \frac{\Gamma(a)\Gamma(b)}{\Gamma(a+b)} \tag{A8}$$

is the beta function.

For the first five space dimensions, relation (A5), for $r \leqslant 2R$, yields

$$\alpha(r;R) = 1 - \frac{r}{2R}, \quad d = 1 \tag{A9}$$

$$\alpha(r;R) = \frac{2}{\pi}\left[\cos^{-1}\left(\frac{r}{2R}\right) - \frac{r}{2R}\left(1 - \frac{r^2}{4R^2}\right)^{1/2}\right], \quad d = 2 \tag{A10}$$

$$\alpha(r;R) = 1 - \frac{3}{4}\frac{r}{R} + \frac{1}{16}\left(\frac{r}{R}\right)^3, \quad d = 3 \tag{A11}$$

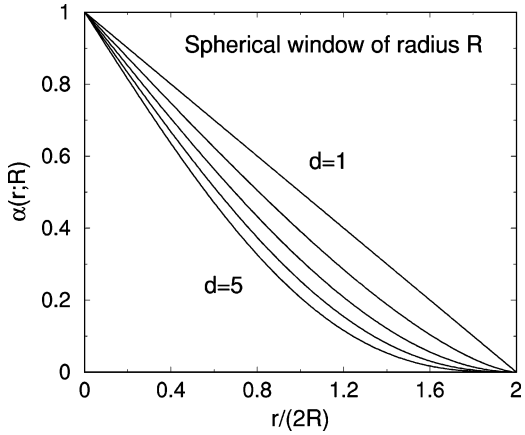

FIG. 9. The scaled intersection volume $\alpha(r;R)$ for spherical windows of radius R as a function of r for the first five space dimensions. The uppermost curve is for $d=1$ and the lowermost curve is for $d=5$.

$$\alpha(r;R)=\frac{2}{\pi}\left[\cos^{-1}\left(\frac{r}{2R}\right)-\left\{\frac{5r}{6R}-\frac{1}{12}\left(\frac{r}{R}\right)^3\right\}\times\left(1-\frac{r^2}{4R^2}\right)^{1/2}\right],\quad d=4 \tag{A12}$$

$$\alpha(r;R)=1-\frac{15}{16}\frac{r}{R}+\frac{5}{32}\left(\frac{r}{R}\right)^3-\frac{3}{256}\left(\frac{r}{R}\right)^5,\quad d=5. \tag{A13}$$

Figure 9 shows graphs of the scaled intersection volume $\alpha(r;R)$ as a function of r for the first five space dimensions. For any dimension, $\alpha(r;R)$ is a monotonically decreasing function of r. At a fixed value of r in the open interval $(0,2R)$, $\alpha(r;R)$ is a monotonically decreasing function of the dimension d.

Expanding the general expression (A5) through first order in r for $r\leqslant 2R$ yields

$$\alpha(r;R)=1-\frac{\Gamma\left(\frac{d}{2}+1\right)}{\Gamma\left(\frac{d+1}{2}\right)\Gamma\left(\frac{1}{2}\right)}\frac{r}{R}+o\left(\frac{r}{R}\right), \tag{A14}$$

where $o(x)$ indicates terms of higher order than x. This relation will be of use to us in developing an asymptotic expression for the number variance for large windows.

APPENDIX B: FLUCTUATIONS IN EQUILIBRIUM HARD-PARTICLE SYSTEMS

Hard particles in equilibrium represent an example of a correlated system that is generally not hyperuniform. The one-dimensional case of identical hard rods of length D in equilibrium is a particularly instructive case because the radial distribution function $g_2(r)$ (in the thermodynamic limit) is known exactly for all densities [52]:

$$\phi g_2(x)=\sum_{k=1}^{\infty}\Theta(x-k)\frac{\phi^k(x-k)^{k-1}}{(1-\phi)^k(k-1)!}\exp\left[-\frac{\phi(x-k)}{1-\phi}\right], \tag{B1}$$

where $x=r/D$ is a dimensionless distance and $\phi=\rho D$ is the covering fraction of the rods, which lies in the closed interval $[0,1]$. Below the close-packed space-filling value of $\phi=1$, the radial distribution function is a short-ranged function in the sense that one can always find a large enough value of r beyond which $g_2(r)$ remains appreciably close to unity. That is, for $\phi<1$, the correlation length is always finite. However, the point $\phi=1$ is singular in the sense that the system exhibits perfect long-range order and thus is hyperuniform. Indeed, at $\phi=1$, the nearest-neighbor distance for each rod is exactly equal to D: a situation that is identically the same as the single-scale one-dimensional periodic point pattern studied in Sec. IV.

Using relation (B1) in conjunction with relations (36) and (37) enables us to compute the ''volume'' and ''surface-area'' contributions to the variance as a function of reduced density ϕ for identical hard rods in equilibrium. The results are summarized in Fig. 10. We see that as the density increases, the volume fluctuations decrease monotonically and only vanish at the space-filling density $\phi=1$: the hyperuniform state. Of course, B vanishes at $\phi=0$ and increases in value as ϕ increases until it achieves a maximum value at $\phi\approx 0.5$. At the hyperuniform state ($\phi=1$), $B=\overline{\Lambda}/2=1/12$, which corresponds to the perfectly ordered close-packed state. For sufficiently small densities, the surface-area coefficient of equilibrium hard-sphere systems in higher dimensions is expected to have the same qualitative behavior as the one-dimensional case. Specifically, the same trends should occur in higher dimensions for densities in the range $0\leqslant\phi\leqslant\phi_f$, where ϕ_f corresponds to the freezing density, i.e., the point above which the system undergoes a disorder to order phase transition. For densities between freezing and melting points, the behavior of the surface-area coefficient is expected to be qualitatively different from that for hard rods in equilibrium, which is devoid of a phase transition. However, we can definitively assert that the highest achievable density along the stable crystal branch is a hyperuniform state. In particular, for hard disks ($d=2$) and hard spheres ($d=3$) in equilibrium, the hyperuniform states correspond to the close-packed triangular lattice and the fcc lattice, respectively.

APPENDIX C: HOW SMALL CAN THE VOLUME COEFFICIENT BE FOR HYPOSURFICIAL SYSTEMS?

We know that a statistically homogeneous and isotropic point pattern cannot simultaneously be hyperuniform and hyposurficial, i.e., the volume coefficient A [cf. Eq. (43)] and surface-area coefficient B [cf. Eq. (44)] both cannot be zero for a strictly convex window (Sec. II C). The purpose of this appendix is to investigate how small A can be made for an infinite hyposurficial point pattern ($B=0$). To that end we consider a hypothetical spherically symmetric pair correlation function $g_2(r)$ and a spherical window. We do not place any additional restrictions on $g_2(r)$ besides the necessary

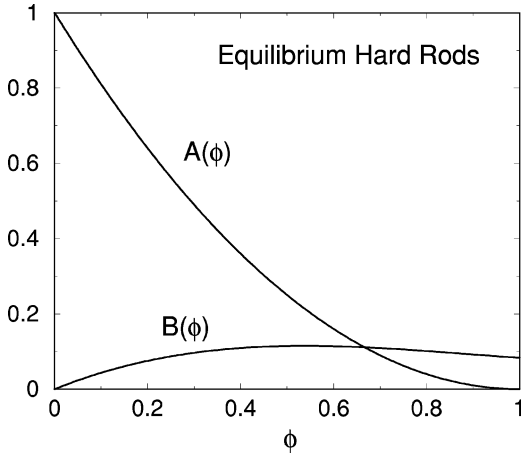

FIG. 10. The volume coefficient $A(\phi)=(1-\phi)^2$ and surface-area coefficient $B(\phi)$ [defined in relation (35)] as a function of the reduced density ϕ for a one-dimensional system of identical hard rods in equilibrium. At the hyperuniform density $\phi=1$, $B=\overline{\Lambda}/2=1/12$, which corresponds to the perfectly ordered close-packed state.

realizability conditions that $g_2(r)\geqslant 0$ for all r and $S(k)\geqslant 0$ for all k. The hypothetical correlation function is characterized by three parameters ϵ, C, and D as follows:

$$g_2(r)=g_S(r)+g_L(r), \tag{C1}$$

where $g_S(r)$ denotes the short-ranged part defined by the step function

$$g_S(r)=\begin{cases}0, & 0\leqslant r\leqslant D\\ 1, & r>D,\end{cases} \tag{C2}$$

and $g_L(r)$ denotes the long-ranged part defined by

$$g_L(r)=\begin{cases}0, & 0\leqslant r\leqslant D\\ C\epsilon\left(\dfrac{D}{r}\right)^{d+1+\epsilon}, & r>D.\end{cases} \tag{C3}$$

Here D is a length parameter, C is a dimensionless constant, and ϵ is a positive ($\epsilon>0$) but small parameter. The necessary condition $g_2(r)\geqslant 0$ requires that the constant C satisfy the trivial inequality

$$C\geqslant -\epsilon^{-1}. \tag{C4}$$

The form of g_2 ensures that we can make the surface-area coefficient B vanish identically, as required. According to relation (44), the surface-area coefficient B is proportional to the dth moment of the total correlation function $h(r)=g_2(r)-1$. The dth moment integral for the hypothetical pair correlation function (C1) is given by

$$\int_0^\infty h(r)r^d dr=-\frac{D^{d+1}}{d+1}+CD^{d+1}. \tag{C5}$$

To make this integral vanish, we take

$$C=\frac{1}{d+1}>0, \tag{C6}$$

which of course satisfies inequality (C4). For such a hyposurficial correlation function (C1) that also satisfies the nonnegativity condition $S(k)\geqslant 0$, we now show that the volume coefficient A is only nonzero by $O(\epsilon^2)$.

Consider volume coefficient A [cf. (38)] with this value of C:

$$A=\lim_{|\mathbf{k}|\to 0}S(\mathbf{k})=1+\rho\int_{\Re^d}h(\mathbf{r})d\mathbf{r}=1-2^d\phi+\left(\frac{2^d d\phi}{d+1}\right)\frac{\epsilon}{1+\epsilon}, \tag{C7}$$

where $\phi=\rho v_1(D/2)$ is a dimensionless density. If one incorrectly sets A to be zero, one finds that the corresponding density is given by

$$\phi_*=\frac{1}{2^d\left(1-\dfrac{d\epsilon}{(d+1)(1+\epsilon)}\right)}. \tag{C8}$$

At such a value of ϕ, however, $S(k)$ will be negative for some $k>0$ near the origin for sufficiently small but nonzero ϵ, which shows in this specific instance that the point pattern corresponding to such a hypothetical g_2 cannot simultaneously be hyperuniform and hyposurficial, as expected. However, one can make $S(k=0)$ positive and very small [while satisfying $S(k)\geqslant 0$ for all k] at a value ϕ slightly smaller than Eq. (C8) in the limit $\epsilon\to 0^+$.

The other necessary condition $S(k)\geqslant 0$ will be obeyed for all k provided that the number density is no larger than some "terminal density" ρ_c (or ϕ_c) [20,40,41]. The structure factor is given by

$$S(k)=1+\rho[H_S(k)+H_L(k)], \tag{C9}$$

where $H_S(k)$ and $H_L(k)$ are the Fourier transforms of $g_S(r)-1$ and $g_L(r)$, respectively. The terminal density is given by

$$\rho_c=-\frac{1}{\min\limits_k[H_S(k)+H_L(k)]}. \tag{C10}$$

For simplicity, we will specialize to the case $d=3$, keeping in mind that our general conclusions apply to arbitrary dimension. Based on the aforementioned arguments, it is sufficient to consider the behavior of $S(k)$ for small k:

$$S(k)=1+8\phi\left[-1+\frac{(kD)^2}{10}-O((kD)^4)\right]+6\phi\frac{\epsilon}{1+\epsilon}$$
$$-\frac{3\phi\sqrt{\pi}\epsilon}{2^{1+\epsilon}(1+\epsilon)}\frac{\Gamma\left(\frac{1}{2}-\frac{\epsilon}{2}\right)}{\Gamma\left(2+\frac{\epsilon}{2}\right)}|kD|^{1+\epsilon}+\frac{\phi\epsilon}{1-\epsilon}(kD)^2$$
$$+O((kD)^4). \tag{C11}$$

The nonanalytic term $|kD|^{1+\epsilon}$ [which arises due to inclusion of relation (C3) for g_L] has the effect of displacing the minimum of $S(k)$ away from the origin when $g_L=0$ to a symmetric pair of locations determined by

$$|k_{min}D| = \frac{15\pi}{16}\epsilon \tag{C12}$$

as $\epsilon \to 0^+$. Moreover, in this leading order

$$S(0) - S(k_{min}) = \frac{45\pi^2\phi}{64}\epsilon^2. \tag{C13}$$

Note that this would lead to an $O(\epsilon^2)$ correction to expression (C8) for ϕ_*. In summary, by adopting the correlation function (C1) with $C=1/(d+1)$, we can make the surface-area coefficient $B=0$ and at the terminal density ϕ_c, the structure factor $S(0)=A$ is only nonzero by $O(\epsilon^2)$.

[1] J.-P. Hansen and I. R. McDonald, *Theory of Simple Liquids* (Academic Press, New York, 1986).

[2] P. J. E. Peebles, *Principles of Physical Cosmology* (Princeton University Press, Princeton, NJ, 1993).

[3] L. Pietronero, A. Gabrielli, and F.S. Labini, Physica A **306**, 395 (2002).

[4] S. Warr and J.-P. Hansen, Europhys. Lett. **36**, 589 (1996).

[5] A. Wax, C. Yang, V. Backman, K. Badizadegan, C.W. Boone, R.R. Dasari, and M.S. Field, Biophys. J. **82**, 2256 (2002).

[6] D.J. Vezzetti, J. Math. Phys. **16**, 31 (1975).

[7] R.M. Ziff, J. Math. Phys. **18**, 1825 (1977).

[8] J.L. Lebowitz, Phys. Rev. A **27**, 1491 (1983).

[9] P.M. Bleher, F.J. Dyson, and J.L. Lebowitz, Phys. Rev. Lett. **71**, 3047 (1993).

[10] T.M. Truskett, S. Torquato, and P.G. Debenedetti, Phys. Rev. E **58**, 7369 (1998).

[11] J. Beck, Acta Math. **159**, 1 (1987).

[12] In very special circumstances, the variance can grow more slowly than the surface area. For example, for the infinite periodic square lattice and when Ω is a rectangle with a very irrational orientation with respect to the x axis, the variance grows as $\ln R$: see J. Beck, Discrete Math. **229**, 29 (2001).

[13] D.G. Kendall, Quarterly J. Math. **19**, 1 (1948).

[14] D.G. Kendall and R.A. Rankin, Quarterly J. Math. **4**, 178 (1953).

[15] S. Torquato, *Random Heterogeneous Materials: Microstructure and Macroscopic Properties* (Springer-Verlag, New York, 2002).

[16] L. D. Landau and E. M. Lifshitz, *Statistical Physics* (Pergamon Press, New York, 1980).

[17] Ph.A. Martin and T. Yalcin, J. Stat. Phys. **22**, 435 (1980).

[18] B. Lu and S. Torquato, J. Chem. Phys. **93**, 3452 (1990).

[19] K. Huang, *Statistical Mechanics* (Wiley, New York, 1987).

[20] S. Torquato and F.H. Stillinger, J. Phys. Chem. B **106**, 8354 (2002); **106**, 11406 (2002). It is interesting to note that for a related two-point correlation function that arises in the characterization of two-phase random media (i.e., binary stochastic spatial processes), it is known that the two analogous nonnegativity conditions are necessary but not sufficient for realizability [15]; see also S. Torquato, J. Chem. Phys. **111**, 8832 (1999).

[21] N. A. C. Cressie, *Statistics for Spatial Data* (Wiley, New York, 1993).

[22] I. N. Sneddon, *Fourier Transforms* (Dover Publications, New York, 1995).

[23] Of course, there may be situations in which $A=0$, but B and/or higher-order moments of h are unbounded. In such instances, the Fourier transform of h will be a nonanalytic function of k at $k=0$.

[24] M. Aizenman, S. Goldstein, and J.L. Lebowitz, J. Stat. Phys. **103**, 601 (2001) have proved that any translation invariant measure in one dimension with bounded variance must be a superposition of periodic measures.

[25] The critical exponent η associated with $h(\mathbf{r})$ for thermal systems belonging to the standard Ising universality class is given exactly by 1/4 for $d=2$ and approximately by 0.05 for $d=3$; see Ref. [19].

[26] M.D. Rintoul and S. Torquato, J. Colloid Interface Sci. **186**, 467 (1997); C.L.Y. Yeong and S. Torquato, Phys. Rev. E **57**, 495 (1998); S. Hyun and S. Torquato, J. Mater. Res. **16**, 280 (2001). These papers are concerned with ''target'' optimization problems in a variety of different contexts.

[27] F.H. Stillinger, P.G. Debenedetti, and S. Sastry, J. Chem. Phys. **109**, 3983 (1998).

[28] *Handbook of Mathematical Functions*, edited by M. Abramowitz and I. A. Stegun (Dover Publications, New York, 1972).

[29] Indeed, this is true for other periodic lattices and for statistically homogeneous point patterns in two and three dimensions. The fact that the asymptotic surface-area coefficient $\overline{\Lambda}$ can be estimated from the average of $\Lambda(R)$ over a small range of R near $R=0$ can be exploited to speed up significantly optimization algorithms to find extremal or targeted values of $\overline{\Lambda}$.

[30] R.A. Rankin, Proc. Glasgow Math. Assoc. **1**, 149 (1953).

[31] E.A. Jagla, J. Chem. Phys. **110**, 451 (1998); Phys. Rev. E **58**, 1478 (1999).

[32] A proof that the extremal lattice for $d=3$ is the bcc lattice currently does not exist. In this connection, it should be noted that the surface-area coefficient for the bcc lattice is related to the Epstein zeta function for the fcc lattice, which was shown [V. Ennola, Proc. Cambridge Philos. Soc. **60**, 855 (1964)] to provide a local minimum value among all lattices.

[33] Of course, the extremal point pattern depends on the shape of the window.

[34] S. Goldstein, E. Speer, and J. L. Lebowitz (unpublished).

[35] A. Gabrielli, B. Jancovici, M. Joyce, J.L. Lebowitz, L. Pietronero, and F.S. Labini, Phys. Rev. D **67**, 043506 (2003).

[36] C. Radin, Ann. Math. **139**, 661 (1994).

[37] D. Levesque, J-J. Weis, and J.L. Lebowitz, J. Stat. Phys. **100**, 209 (2000).

[38] B. Jancovici, Phys. Rev. Lett. **46**, 386 (1980).

[39] E.R. Harrison, Phys. Rev. D **1**, 2726 (1970); Ya.B. Zeldovich,

Mon. Not. R. Astron. Soc. **160**, 1 (1972).
[40] F.H. Stillinger, S. Torquato, J.M. Eroles, and T.M. Truskett, J. Phys. Chem. B **105**, 6592 (2000).
[41] H. Sakai, F.H. Stillinger, and S. Torquato, J. Chem. Phys. **117**, 297 (2002).
[42] S. Torquato, T.M. Truskett, and P.G. Debenedetti, Phys. Rev. Lett. **84**, 2064 (2000).
[43] A.R. Kansal, S. Torquato, and F.H. Stillinger, Phys. Rev. E **66**, 041109 (2002).
[44] S. Torquato and F.H. Stillinger, J. Phys. Chem. B **105**, 11849 (2001); S. Torquato, A. Donev, and F. H. Stillinger, Int. J. Solids Struct. **40**, 7143 (2003).
[45] J. Crawford, S. Torquato, and F. H. Stillinger, J. Chem. Phys. **119**, 7065 (2003).
[46] It is an open question whether the triangular lattice and the body-centered cubic lattice correspond to the global minimum value of $\overline{\Lambda}/\phi^{(d-1)/d}$ among all infinite hyperuniform point patterns in two and three dimensions, respectively, for spherical windows.
[47] A.R. Kansal, S. Torquato, and F.H. Stillinger, J. Chem. Phys. **117**, 8212 (2002).
[48] D. Levine and P.J. Steinhardt, Phys. Rev. B **34**, 596 (1986).
[49] J.M. Kosterlitz and D.J. Thouless, J. Phys. C **6**, 1181 (1973); B.I. Halperin and D.R. Nelson, Phys. Rev. Lett. **41**, 121 (1978); A.P. Young, Phys. Rev. B **19**, 1855 (1979).
[50] F.H. Stillinger and R. Lovett, J. Chem. Phys. **48**, 3858 (1968).
[51] Y. Fan, J.K. Percus, D.K. Stillinger, and F.H. Stillinger, Phys. Rev. A **44**, 2394 (1991).
[52] F. Zernike and J.A. Prins, Z. Phys. **41**, 184 (1927).